



HAL
open science

Development of cortical folds in the human brain: An attempt to review biological hypotheses, early neuroimaging investigations and functional correlates

Héloïse de Vareilles, D Rivière, J F Mangin, J Dubois

► To cite this version:

Héloïse de Vareilles, D Rivière, J F Mangin, J Dubois. Development of cortical folds in the human brain: An attempt to review biological hypotheses, early neuroimaging investigations and functional correlates. *Developmental Cognitive Neuroscience*, 2023, 61, 10.1016/j.dcn.2023.101249 . hal-04277201

HAL Id: hal-04277201

<https://hal.science/hal-04277201>

Submitted on 9 Nov 2023

HAL is a multi-disciplinary open access archive for the deposit and dissemination of scientific research documents, whether they are published or not. The documents may come from teaching and research institutions in France or abroad, or from public or private research centers.

L'archive ouverte pluridisciplinaire **HAL**, est destinée au dépôt et à la diffusion de documents scientifiques de niveau recherche, publiés ou non, émanant des établissements d'enseignement et de recherche français ou étrangers, des laboratoires publics ou privés.



Development of cortical folds in the human brain: An attempt to review biological hypotheses, early neuroimaging investigations and functional correlates[☆]

H. de Vareilles^{a,*}, D. Rivière^a, JF Mangin^a, J. Dubois^{b,c}

^a Université Paris-Saclay, NeuroSpin-BAOBAB, CEA, CNRS, Gif-sur-Yvette, France

^b Université Paris Cité, NeuroDiderot, Inserm, Paris, France

^c Université Paris-Saclay, NeuroSpin-UNIACT, CEA, Gif-sur-Yvette, France

ARTICLE INFO

Keywords:

Sulcus
Gyrification
Fetuses
Neonates
Prematurity
MRI

ABSTRACT

The folding of the human brain mostly takes place in utero, making it challenging to study. After a few pioneer studies looking into it in post-mortem foetal specimen, modern approaches based on neuroimaging have allowed the community to investigate the folding process in vivo, its normal progression, its early disturbances, and its relationship to later functional outcomes. In this review article, we aimed to first give an overview of the current hypotheses on the mechanisms governing cortical folding. After describing the methodological difficulties raised by its study in fetuses, neonates and infants with magnetic resonance imaging (MRI), we reported our current understanding of sulcal pattern emergence in the developing brain. We then highlighted the functional relevance of early sulcal development, through recent insights about hemispheric asymmetries and early factors influencing this dynamic such as prematurity. Finally, we outlined how longitudinal studies have started to relate early folding markers and the child's sensorimotor and cognitive outcome. Through this review, we hope to raise awareness on the potential of studying early sulcal patterns both from a fundamental and clinical perspective, as a window into early neurodevelopment and plasticity in relation to growth in utero and postnatal environment of the child.

1. Introduction

A notorious characteristic of the human brain is its involuted shape, displaying ridges (gyri) and furrows (sulci). The resulting pattern is globally stable across individuals, which allows us to identify analogue sulci within the population and to compare them. Yet, even though one can identify the same sulcus in two different brains, the shape and orientation of this sulcus will differ. This calls for an investigation of the variability of cortical folding and its significance. Historically, the study of cortical folds was undertaken in the context of descriptive anatomy (e.g. Cunningham, 1892), and it is still nowadays investigated in this light, with advances in neuroimaging now allowing in vivo observations, with more reliable measures on larger cohorts (e.g. Sprung-Much and Petrides, 2018).

Since a few years, the study of sulci has taken a new turn, once again thanks to the advancement of neuroimaging, with the consideration of links between sulcal pattern and functional activations: many cerebral responses have been located in specific anatomical regions, which may themselves be constrained by gyral and sulcal patterns. The inter-individual folding variability (as illustrated in Fig. 1, along with an atlas of folds (Borne, 2019) with the nomenclature used in this review, detailed in Table 1) might then partly explain the variability observed in functional activations across subjects. Such potential links evidenced the importance of taking the folding variability into account for inter-subject alignment to match analogous functional regions in different brains (for review, see Mangin et al., 2015a; Mangin et al., 2016). This also led to an effort in the search for anatomo-functional correlates. Recently, some links have been demonstrated between

Abbreviations: IUGR, intra-uterine growth restriction; IVH, intraventricular haemorrhage; MRI, magnetic resonance imaging; SPANGY, spectral analysis of gyrification; TEA, term-equivalent age; w GA, weeks of gestational age; w PMA, weeks of post-menstrual age.

[☆] Article for Developmental Cognitive Neuroscience, February 14th, 2023

* Correspondence to: CEA/SAC/DRF/Institut Joliot/NeuroSpin/BAOBAB, Bât 145, point courrier 156, 91191 Gif-sur-Yvette, France.

E-mail address: heloise.devareilles@protonmail.com (H. de Vareilles).

<https://doi.org/10.1016/j.dcn.2023.101249>

Received 14 October 2022; Received in revised form 28 March 2023; Accepted 21 April 2023

Available online 25 April 2023

1878-9293/© 2023 The Authors. Published by Elsevier Ltd. This is an open access article under the CC BY-NC-ND license (<http://creativecommons.org/licenses/by-nc-nd/4.0/>).

sulcation and brain function, cognition and behaviour (for review, see Jiang et al., 2021), and, in some specific regions, linked sulcal pattern to the localization of functional activations, as for example the location of activations for hand movements and silent reading in relation to the shape of the central sulcus (Sun et al., 2016). This raises questions about whether the formation of folds might be related to the emerging functional specialization during development.

Before diving in the core subject of the current review, the development of cortical folds, let us address some fundamentals about the folded brain. In terms of general post-natal development of the brain, an interesting concept was inferred from a comparison including macaques, human term-born infants, and adults (Hill et al., 2010). It pointed out that regional expansion of cortical surface area is similar during human development and primate evolution, and consequently suggested that regions of recent evolutionary expansion may benefit from maturing after birth, either for post-natal environment integration, or to prioritize early-life resources on regions optimizing early-life survival. This study was an elegant example of the use of comparative description of brain features between different species to gain insights on the human brain development, and this concept has also been applied to the evolution of cortical folding across species (for review, see Zilles et al., 2013; Van Essen et al., 2019).

In terms of general considerations on the folding of the human brain, a first global observation is that the degree of gyrification scales with brain size. Larger brains show more augmentation in surface area than in cortical thickness following an allometric scaling law, showing more folds (Im et al., 2008; Germanaud et al., 2012). Moreover, globally the sulcal pattern remains stable during the lifespan, with only minor changes reported during childhood (Blanton et al., 2001). During adolescence, the cortex flattens, mostly in the frontal and occipital cortices (Aleman-Gomez et al., 2013). During adulthood, sulci widen and become shallower with age, more importantly in men for a set of sulci (Kochunov et al., 2005). Yet, this does not seem to affect significantly the sulcal patterns that appear early on; a striking example is the longitudinal stability of the pattern of a variable tertiary sulcus – namely the paracingulate sulcus – which was reported to be fixed in every single subjects from 7 to 32 years of age (Cachia et al., 2016).

This longitudinal stability of folding patterns erects sulcal pattern as a lead macroscopic anatomical proxy for *in utero* development (Mangin et al., 2010; Cachia et al., 2021). In this sense, sulcal pattern has been reported to correlate to prenatal dispositions to cognition (e.g. the pattern of the occipitotemporal sulcus relates with reading accuracy; Cachia et al., 2018), response to later-life neurological adversities (e.g. the pattern of orbitofrontal sulci is related to transition to psychosis in at-risk patients; Lavoie et al., 2014), and flat-out developmental anomalies in links with pathologies (e.g. congenital one handers show a significantly flatter central sulcus contralateral to the absent limb than for acquired amputation and control situations; Sun et al., 2017).

The use for sulcal pattern as a proxy for *in utero* development makes it crucial to have a clear understanding of why, how and when the different cortical folds emerge, and their relation to function. We therefore attempt to review the different elements of answer to these questions. In a first part, we describe our current understanding of the mechanisms at play, as well as the progression of cortical folding in the developing brain after having summarized the complexities of early-life MRI studies. In a second step, we highlight the possible links between sulcation and function development at a very early age, first through asymmetry studies, then considering early deviations in folding, and finally looking into longitudinal development studies in preterm infants.

2. Folding mechanisms and progression in the human brain

2.1. Folding mechanisms

A number of different scientific fields have tried to understand why the brain folds for certain but not all mammals and have brought to light concurring mechanisms. Before assessing their causes, let us differentiate two different types of folding: opercularization and sulcation. Opercularization is due to a greater development of the frontal, parietal and temporal lobes compared to the insular lobe, inducing a folding of these regions over the insula (implying that the frontal and parietal lobes become neighbours to the temporal lobe, over the insula), and resulting in the Sylvian Fissure. On the reverse, sulcation per se seems to be due to intricate cellular phenomena inducing a mechanical buckling within a

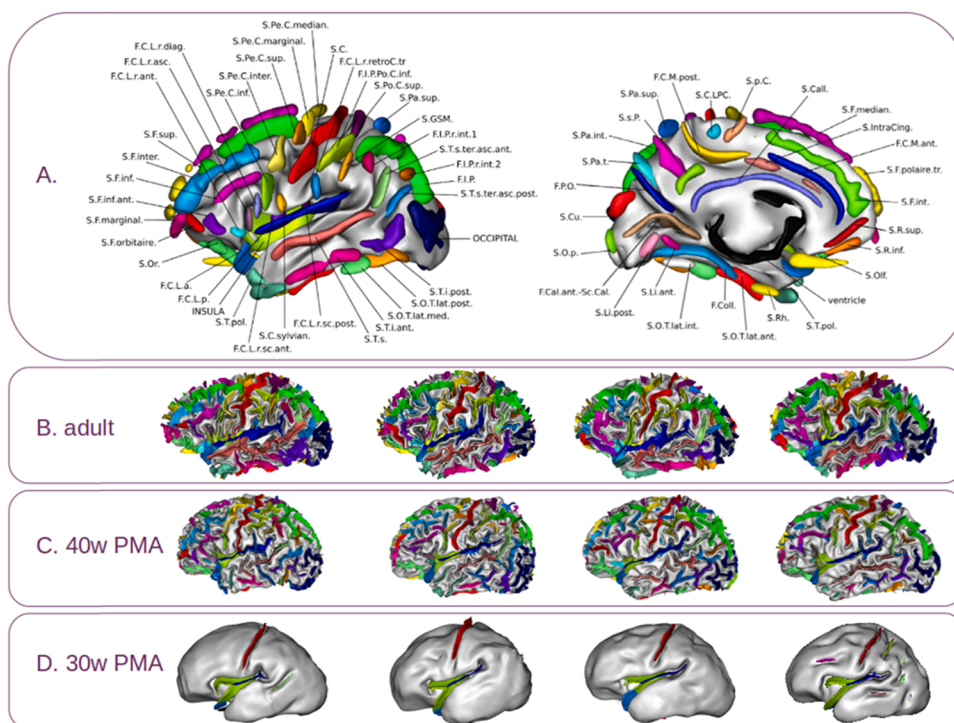


Fig. 1. A. Nomenclature of sulcal objects (Borne, 2019) represented on a thresholded statistical probabilistic anatomy map (Perrot et al., 2011) of a lateral (left) and medial (right) view of a left hemisphere (see Table 1 for detailed sulcal names). B-D. Lateral view of labelled left hemispheres (B. in four adults, C. in four preterm infants, at 40 weeks of post-menstrual age (w PMA) and D. in the same preterm infants, at 30w PMA). All figures were generated using the BrainVISA software (<https://brainvisa.info>).

Table 1
Detailed names for sulci and fissures in Fig. 1.A.

acronym	sulcus/fissure name
F.C.L.a.	anterior Sylvian fissure
F.C.L.p.	posterior Sylvian fissure
F.C.L.r.ant.	anterior ramus of the Sylvian fissure
F.C.L.r.asc.	ascending ramus of the Sylvian fissure
F.C.L.r.diag.	diagonal ramus of the Sylvian fissure
F.C.L.r.retroC.tr.	transverse retrocentral ramus of the Sylvian fissure
F.C.L.r.sc.ant.	anterior sub-central ramus of the Sylvian fissure
F.C.L.r.sc.post.	posterior sub-central ramus of the Sylvian fissure
F.C.M.ant.	anterior cingulate sulcus
F.C.M.post.	posterior cingulate sulcus
F.Cal.ant.-Sc. Cal.	calcarine sulcus
F.Coll.	collateral sulcus
F.I.P.	intraparietal sulcus
F.I.P.Po.C.inf.	inferior postcentral sulcus
F.I.P.r.int.1	first interior ramus of the intraparietal sulcus
F.I.P.r.int.2	second interior ramus of the intraparietal sulcus
F.P.O.	occipitoparietal sulcus
INSULA	insula
OCCIPITAL	occipital sulci
S.C.	central sulcus
S.C.LPC.	paracentral lobule central sulcus
S.C.Sylvian.	central Sylvian sulcus
S.Call.	subcallosal sulcus
S.Cu.	cuneal sulcus
S.F.inf.	inferior frontal sulcus
S.F.inf.ant.	anterior inferior frontal sulcus
S.F.int.	internal frontal sulcus
S.F.inter.	intermediate frontal sulcus
S.F.marginal.	marginal frontal sulcus
S.F.median.	median frontal sulcus
S.F.orbitaire.	frontal orbary sulcus
S.F.polaire.tr.	transverse polar frontal sulcus
S.F.sup.	superior frontal sulcus
S.GSM.	sulcus of the supra-marginal gyrus
S.intraCing.	intra-lingulate sulcus
S.Li.ant.	anterior intralingual sulcus
S.Li.post.	posterior intralingual sulcus
S.O.p.	occipitopolar sulcus
S.O.T.lat.ant.	anterior lateral occipitotemporal sulcus
S.O.T.lat.int.	internal occipitotemporal sulcus
S.O.T.lat.med.	medium lateral occipito-temporal sulcus
S.O.T.lat.post.	posterior lateral occipito-temporal sulcus
S.Olf	olfactive sulcus
S.Or.	orbital sulcus
S.p.C.	paracentral sulcus
S.Pa.int.	internal parietal sulcus
S.Pa.sup.	superior parietal sulcus
S.Pa.sup.	superior parietal sulcus
S.Pa.t.	transverse parietal sulcus
S.Pe.C.inf.	inferior precentral sulcus
S.Pe.C.inter.	intermediate precentral sulcus
S.Pe.C.marginal.	marginal precentral sulcus
S.Pe.C.median.	median precentral sulcus
S.Pe.C.sup.	superior precentral sulcus
S.Po.C.sup.	superior postcentral sulcus
S.R.inf.	inferior rostral sulcus
S.R.sup.	superior rostral sulcus
S.Rh.	rhinal sulcus
S.	sub-parietal sulcus
S.T.i.ant.	anterior inferior temporal sulcus
S.T.i.post	posterior inferior temporal sulcus
S.T.pol.	polar temporal sulcus
S.T.pol.	polar temporal sulcus
S.T.s.	superior temporal sulcus
S.T.s.ter.asc.ant.	anterior terminal ascending branch of the superior temporal sulcus
S.T.s.ter.asc. post.	posterior terminal ascending branch of the superior temporal sulcus
ventricle	ventricle

given region, resulting in the apparition of sulci.

As detailed in the next sections, cellular biology, genetics and biomechanics have proposed different models to describe and explain these folding mechanisms, initially investigated separately and summarized here in order to gain a better overall understanding of the process.

2.1.1. Cellular biology

In terms of cellular biology, a comprehensive review precisely depicted the detailed organization of the foetal and neonatal brain (Kostović et al., 2019). Here, we focus on processes which are directly linked to cortical folding. A first observation is that in the mature brain, the cortex is thicker in gyral crests and thinner in sulcal fundi. The morphology and distribution of the cortex's components differ between crests and fundi: in crests, the "column and layer" neuronal organization is more precise, the density of cell bodies is lower, the myelinated fibres are denser, oriented more vertically, and the pyramidal neurons show a vertically oriented configuration, with longer and more elaborated dendrites than their counterparts in sulcal fundi (Llinares-Benadero and Borrell, 2019). In gyrencephalic species, these specificities arise from the multiple neurogenetic events concurring in the developing brain, including neuronal and glial cell proliferation and migration. Regarding proliferation, in the ferret, a heterogeneous rate of neurogenesis has been reported in the basal germinal zones, inducing, in the developing cortical plate, regions of higher neuronal density and regions of lower neuronal density. These were reported to respectively match future gyral crests and future sulcal fundi, eventually resulting in a homogeneous neuronal density across the cortex in the mature brain, due to more folding and area expansion in the higher neuronal density regions (Rockel et al., 1980). Migration is also an important factor in sulcation: the inhibition of intercellular adhesion of migrating cortical neurons induces folding without progenitor cell amplification in mice (a normally lissencephalic species), while preserving layered organization and radial glial morphology (del Toro et al., 2017). Incidentally, a recent review article has assessed different animal models with induced cortical folding and differentiated the ones which resulted in realistic folding properties from those which did not (Borrell, 2018). Radial glial cells, which guide the migration of neurons from the ventricular and subventricular proliferative zones to the cortical mantle, also seem involved in cortical folding: in lissencephalic species, the radial glial cells are parallel, while they are distributed in a heterogeneous manner in gyrencephalic species, with fan-shaped configurations in the regions undergoing greater folding expansion inducing a greater tangential expansion of radially migrating neurons (Llinares-Benadero and Borrell, 2019). This divergence of radial glial cells can be linked to the relative abundance of basal radial glial cells in gyrencephalic species compared to lissencephalic ones, whose cell somas are located both in the inner and outer subventricular zones where they undergo mitosis. The large number of basal glial cells, which extend their basal fibre in the pre-existing radial glial scaffold, cause a divergence in it (Fig. 2. A). A recent review further suggested that the subplate (a transient layer of neurons between the cortical plate and the intermediate zone – future white matter, Fig. 2. B) may drive cortical folding through directional cues to guide fibres (Rana et al., 2019).

2.1.2. Genetics

These biological events seem to be thoroughly genetically constrained. For example, as mentioned above, the ferret brain shows heterogeneous neurogenesis rates along the germinal layers which seem to match the future location of sulci and gyri: genetic patterning has concurrently been observed, with specific genes displaying similarly heterogeneous degrees of expression which matched future folds, and which were associated to differences in proliferation and neuronal migration (Llinares-Benadero and Borrell, 2019). In link to the opercularization mechanism, in the human, it was reported that the frontal, parietal and temporal lobes show differences in transcriptome compared

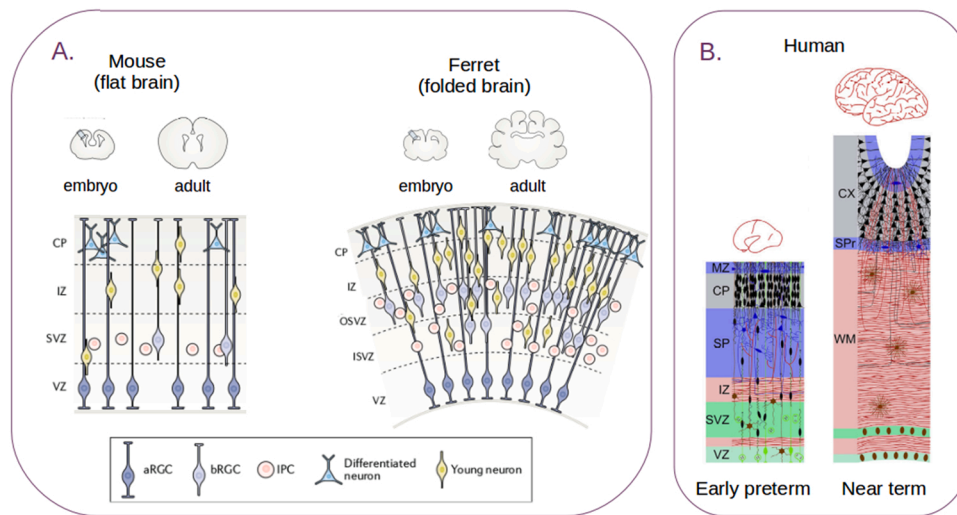


Fig. 2. Illustration of cellular organisation and compartments during cortical development and resulting gyrification A. in the mouse and the ferret at the embryonic stage (courtesy of [Llinares-Benadero and Borrell, 2019](#)), and in B. in the human at the early preterm and near term stages (courtesy of [Kostović et al., 2019](#)). aRGC: apical radial glial cell; bRGC: basal radial glial cell; CP: cortical plate; CX: cortex; IPC: intermediate progenitor cell; ISVZ: inner subventricular zone; IZ: intermediate zone; MZ: marginal zone; OSVZ: outer subventricular zone; SP: subplate; SVZ: subventricular zone; VZ: ventricular zone; WM: white matter.

to the insula, including genes related to neuronal proliferation and differentiation ([Mallela et al., 2020](#)). The ratio between subplate and cortical plate thicknesses during foetal development has been correlated to regional gene expression levels ([Vasung et al., 2021](#)). These are refined clues that genetics and cellular mechanisms linked to folding are intertwined. Previously, less refined clues suggested the implication of genetics in cortical folding. For example, in pathology, an association has been reported between bilateral frontoparietal polymicrogyria (inducing abnormally small and numerous gyri in the frontal and parietal regions) and the mutation of a given gene encoding a G-protein coupled receptor ([Piao et al., 2004](#)). In the general population, males have been reported to show longer sulci than females after correcting for brain size (while sex chromosome dosage did not show specific impacts on overall folding architecture; [Fish et al., 2016](#)).

More generally, the genetic heritability of various sulcal metrics has been tested, which led to the conclusion that earlier forming sulci show higher heritability and that the most heritable sulcal metric is sulcal width, at least during ageing ([Pizzagalli et al., 2020](#)). Although these different results suggested some genetic implication in cortical folding, it seems far from explaining the complexity of sulcal shape: when comparing monozygotic twins to dizygotic twins, it was observed that while brain size is highly heritable, the heritability of sulcal pattern is lower, even though monozygotic twins show more similar patterns than dizygotic twins ([Bartley et al., 1997](#)). The higher sulcal similarity between monozygotic twins have been reproduced comparing them to unrelated pairs of subjects using sulcal graph matching based on sulcal pits ([Im et al., 2011](#)) (as discussed below, these pits are local depth maxima of sulcal basins, identified by watershed algorithms; [Mangin et al., 2015b](#)). It is interesting to assess genetic constraints using such a model, since sulcal pits or roots have been hypothesized to be anatomical correlates of the “protomap” folding model, according to which the early cells of the embryonic vesicle carry their intrinsic program for species-specific cerebral regionalization (protomap: [Rakic, 1988](#); link to sulcal roots: [Régis et al., 2005](#)). To go further, the heritability of deep sulcal pits has been tested, and it was shown to have some small yet relevant symmetric genetic influences on the left and right hemispheres ([Le Guen et al., 2018](#)). Moreover, this study reported a specific heritability asymmetry across the two hemispheres, in the superior temporal sulcus, with the left one being more genetically constrained. Further investigation found an association between the anatomy of superior temporal regions and a given genomic region, in the depth of the left superior temporal asymmetrical pit ([Le Guen et al., 2019](#)). A recent review focusing on sulcal pits and the developing brain suggested a link between the stability of sulcal pits distribution and the stability of the human-specific protomap ([Im and Grant, 2019](#)). From this corpus of

evidence, we can conclude that genetic influence is crucial for the formation of folds, but not sufficient to explain the variability of folding patterns in the human brain.

2.1.3. Biomechanics

The missing piece of the puzzle is perhaps biomechanics. Diverse biomechanical models considering different tissues with different viscoelastic properties have been proposed to simulate cortical folding, and recent models have highlighted that changing some parameters (such as initial geometry, or cortical thickness) induce folding variations which can both justify intra and inter-species variability. A number of reviews have discussed the different models in relation to supporting or opposing evidence from a number of fields, including animal, physical mathematics, and computational models ([Toro and Burnod, 2005](#); [Bayly et al., 2014](#); [Garcia et al., 2018a](#); [Kroenke and Bayly, 2018](#); [Foubet et al., 2019](#); [Heuer and Toro, 2019](#); [Van Essen, 2020](#)). We tried to summarize these different theories here.

In computational modelling of brain folding, the classic approach is to consider the brain before sulcation as composed of two layers: the outer layer representing the cortical plate, and the inner layer representing the tissue between the cortical plate and the proliferative ventricular surface, i.e. the intermediate zone ([Kroenke and Bayly, 2018](#)). Models for cortical folding can be dichotomized between those which consider that the governing forces arise from either the outer or the inner layer. A first model of outer-layer governing forces is based in the hypothesis that the skull and meninges constrained the outer expansion of the cortex, forcing it to fold in order to fit in its container. This hypothesis was disproved, notably through the observation of gyration after relieving cranial pressure in cats ([Welker, 1990](#)). Another outer-layer governing forces model relies on the hypothesis that the tangential expansion is greater for the outer zone than for the inner zone, inducing a mechanical buckling which results in cortical folding ([Toro and Burnod, 2005](#)). Contrarily to the former hypothesis, this hypothesis is supported by biophysical models using swelling gels ([Tallinen et al., 2014](#); [Tallinen et al., 2016](#)) and numerical simulations ([Xu et al., 2010](#); [Tallinen et al., 2016](#)). By building a smooth brain mimic with either layered gels or simulation (using quantitative measurable parameters), and expanding the outer layer (by swelling for gels) faster than the inner layer, the resulting convolutions resemble the folding of the developing brain ([Tallinen et al., 2016](#)). The consistency of this hypothesis and experimental results pushed further investigation on how different parameters of such models imply variations in sulcation which concur with observations, including stiffness, growth rate, initial cortical plate thickness, and initial geometry ([Wang et al., 2019](#); [Wang et al., 2021](#)). Independently from the two-layer model, additional

computational efforts have been deployed to model the variability of brain folding pattern through reaction-diffusion mechanisms based on Turing morphogens to mimic the differential growth of sulci and gyri (Lefevre and Mangin, 2010). This model resulted in developmentally consistent patterning of the brain and in variations in sulcal pattern matching some observed in real-life (such as sulcal interruptions).

In terms of inner-layer governing forces, a first hypothesis was that radial growth of the inner zone occurs at different rates, and that gyri arise from more growth of the inner zone than in sulci. This has been disproved: if gyri were formed by the inner zone pushing the outer zone outwards, a compressive radial force should arise at the centre of gyri, while a tensile force has been observed (Xu et al., 2010). Another inner-zone governing forces theory, more popular than the previous one, relies on the hypothesis of axonal tension. The seminal article suggested that the tension along axons pulled the sulcal walls together, inducing folds by pulling together strongly connected cortical regions while allowing more weakly connected regions to drift apart (Van Essen, 1997). Axonal tension has indeed been reported in the developing ferret brain, yet not in the direction which would induce folding (Xu et al., 2010), apparently disproving the axon tension hypothesis. Nevertheless, an updated version of the tension-based morphogenesis has been proposed with the “differential expansion sandwich plus” (Van Essen, 2020), which offers to solve the apparent contradiction between tension-based models and experimental observations. In it, the contribution of different cells and different cortical and subcortical layers to the folding of the brain are detailed, inducing either radial, tangential or pathway-specific tension depending on the type of cell and region. All in all, the role of white matter in cortical folding is most likely complex and should not be overlooked.

These biomechanical models greatly inform on folding mechanisms, but do not seem to be sufficient by themselves to account for the complexity of the phenomenon as well as the similarities and dissimilarities observed across individual brains. Indeed, these biomechanical models have to be parametrized based on biological phenomena (and, by extension, on genetic ones), both for initial conditions and dynamics. In any case, biomechanical forces may fill in the last brick of cortical folding dynamics, with plausible causes for inter-individual variability. Yet, it should not be reduced to the final brick, coming after cellular and genetic considerations, since all three are deeply intertwined: mechanical forces, in turn, affect cellular activity. Biological forces affect geometry through mechanical stress, impacting the pathways of morphogens and signalling molecules (Foubet et al., 2019; Heuer and Toro, 2019).

Therefore, even though at first, these different fields were brought together mainly to validate or invalidate a given model based on its compatibility with the other fields, it appears that the mechanisms are not only concurrent but also interactive, and recent reviews advocate the combination of the three domains to understand the complex mechanisms at play. Among them, some have focused on the combination of cellular biology and biomechanics (Lewitus et al., 2013; Ronan and Fletcher, 2015; Striedter et al., 2015), including a dual perspective review with both a cellular biology (Borrell, 2018) and a biomechanistic (Kroenke and Bayly, 2018) point of view, with comments from the other perspective. Others have rather focused on the combination between cellular biology and genetic processes, which seem to orchestrate the biological events leading to cortical folding (Sur and Rubenstein, 2005). More recent reviews have combined the three approaches for a more global understanding of the overall folding mechanisms (Fernández et al., 2016; Llinares-Benadero and Borrell, 2019). All in all, these models become meaningful when confronted to in-vivo observations. Refined in-vivo imaging of the human brain is currently best achieved through magnetic resonance imaging (MRI), especially during development. It should be noted that it is not the exclusive means of anatomical imaging in these populations, as, for example, ultrasound allows sulcal investigation to some extent, though limited (Ginsberg et al., 2021). Nevertheless, MRI-based developmental analyses require

specific methodological implementations because of the many hurdles in acquisition and processing of fetal and neonatal MRI.

2.2. Investigating early cortical folding through MRI

Now that we have clarified the current understanding of the folding mechanisms, we aim to address the difficulties of studying sulcation in vivo in the fetus, newborn (post-natal age below 28 days) or infant (below 1 year of age) through the means of MRI. Recent reviews have brilliantly assessed the situation and explored the limits and perspective of early-life neuroimaging (Vasung et al., 2019; Li et al., 2019; Dubois et al., 2021), with the second one focusing more on computational developments to adapt methodologies implemented for the adult brains to the infant brain. In order to summarize the difficulties arising from the study of early folding, we here highlight some considerations regarding acquisition and processing of MRI data, and some ulterior computational methods which have required methodological adaptations.

2.2.1. MRI acquisition and processing

The first hurdle to overcome is MRI acquisition, most complex in the fetus, but also challenging in the neonate and in the infant (cf. Table 2. A). Then, it is necessary to reconstruct the image, to compensate for low image spatial resolution relatively to the brain structure size and to correct motion-related artefacts particularly in fetus images resulting from fast multi-slice imaging (cf. Table 2. B).

After that, the MRI images need to be segmented to allow analyses, by differentiating the different components of the image into supposed cerebral tissues (such as grey matter, white matter and cerebrospinal fluid) and structures (e.g. lobes, sub-cortical structures) based on their contrasts, morphology and sometimes location. Segmentation can be operated manually, yet to gain time and improve consistency and reproducibility in group studies, automatic segmentation methods are required, both in the fetus and neonate (cf. Table 2. C; for review, see: Makropoulos et al., 2018b). An interesting way to compare such methods is through benchmarks: the NeoBrainS12 challenge proposed comparisons of various methods cited here, among others, based on images acquired on preterm infants at 30 and 40 weeks of post-menstrual age (w PMA) (İşgum et al., 2015). A recent article proposing an open dataset of manually segmented foetal brains (including healthy and pathological subjects) also offered a benchmark of ten different segmentation algorithms which were produced by four different teams, and which included a multi-atlas segmentation approach along with a number of deep learning approaches, based on multiple 2D U-Nets, 3D U-Nets, or mask R-CNN deep neural networks (Payette et al., 2021).

The resulting segmentations allow the extraction of different objects and measures useful for subsequent analyses, including cortical surfaces necessary for sulcal detection. Sulcal analysis can be apprehended on either a whole brain or regional level (which are further qualified as global approaches), or in a sulcus-specific approach, in which case the sulcus of interest has to be identified prior to the analysis. In global approaches, curvature-based methods allow a parametrization of folding to assess inter-individual differences (e.g. Luders et al., 2006; Boucher et al., 2009). In the very young brain, sulcal detection is challenging because of its rather smooth configuration in its early developmental stages. Before even assessing sulcal metric, this can make it challenging to define borders for region-wise analyses (cf. Table 2. D). In sulcus-specific approaches, their detection, usually based on local curvature properties (Dubois et al., 2008a), can be biased by acquisition noise, and classic object-based approaches used in the adult are not always suitable. For example, in the adult, the sulcal pits approach is based on such curvature properties, with sulcal pits defined as the local depth maxima of sulcal basins, in order to provide more stable landmarks than sulci (Fig. 3. A; Lohmann et al., 2008; Im et al., 2010). It is particularly interesting to evaluate sulcal pits in the very young brain, as the sulcal pits are closely related to the sulcal roots model, which

Table 2

Overview of methods to overcome technical difficulties in the analysis of early-life MRI data for brain folding explorations.

MRI step	Technical difficulties	Method	References (non-exhaustive list)
A. Image acquisition	Fetus in the womb: angle of acquisition, field of view, mother's tissues, fetal movements, mother's breathing Brain structure size relatively to image spatial resolution Contrast changing with maturation	Ultra-short imaging sequences of T2-weighted images	<i>Reviews:</i> Fetus: Studholme (2015) Fetus, neonate and infant: Dubois et al. (2014)
B. Image reconstruction	Head movements Low spatial resolution compared with brain size	Motion correction Inhomogeneities correction Super-resolution	Fetus: Rousseau et al. (2006); Gholipour et al. (2011); Kuklisova-Murgasova et al. (2012); Rousseau et al. (2013) Neonate: Cordero-Grande et al. (2018); Makropoulos et al. (2018a)
C. Segmentation of brain tissues	Head movements Low spatial resolution Contrast changing with maturation	Atlas-based segmentation relying on spatial registration	Fetus: Habas et al. (2010) Preterm infant: Cardoso et al. (2013); Kim et al. (2016b); Liu et al. (2016) TEA preterm infant: Anbeek et al. (2013); Makropoulos et al. (2014) Term-born neonate: Prastawa et al. (2005); Shi et al. (2010); Wang et al. (2011); Wang et al. (2015); Bae et al. (2021)
D. Brain parcellation	Brain too smooth so little sulcal landmarks between anatomical regions	Intensity-based segmentation with topological constraints	Fetus: Gholipour et al. (2011) Preterm infant: Dubois et al. (2008a); Moeskops et al. (2015) Term-born neonate: Hill et al. (2010); Leroy et al. (2011); Gui et al. (2012)
		Deep-learning benchmark	Fetus: Payette et al. (2021) Infants: Zhao et al. (2022)
		Intrinsic geometric information	Fetus: Lefèvre et al. (2018)
E. Sulcal detection	Folds barely deepened so difficult to detect given the image spatial resolution	Evolution of cortical parameters	Fetus: Xia et al. (2019)
		Atlas-based	Term-born neonate: Adamson et al. (2020)
F. Automated sulcal identification	Brain and region size, intensity and localization of sulcation changing with age	Local curvature properties Adjusting parameters	Fetus: Im and Grant (2019); Auzias et al. (2015) Preterm infant: Dubois et al. (2008a), Bouyeure et al. (2017) Term-born neonate: Meng et al. (2018)
G. Registration	Anatomical landmarks missing	Use of foetal atlas Local curvature properties	Fetus: Yun et al. (2019)
		Volumetric group-wise registration	Fetus: Habas et al. (2012)
		Sulcal matching	Preterm, term and adult: Leberberg et al. (2018) Fetus: Auzias et al. (2015) Preterm and TEA preterm: Orasanu et al. (2016)
		Spectral surface matching	Fetus: Wright et al. (2015)
		Multi-modal surface matching	Preterm and term-born infants: Robinson et al. (2018) Preterm infants (longitudinal): Garcia et al. (2018b)

TEA: term-equivalent age

hypothesises that sulcation develops from stable elementary folds appearing during the foetal stage, with sulci resulting from the merging of these stable elementary folds (Cachia et al., 2003; Régis et al., 2005; Auzias et al., 2015). Yet, for sulcal pit extraction in term-born neonates, the changes in brain size prevent from using fixed threshold parameters, as in the adult (cf. Table 2. E).

For sulcus-specific approaches, as suggested above, an additional difficulty lies in *labelling* of the sulci to isolate the object of interest. In the adult, manual labelling by trained expert based on reference atlases (Ono et al., 1990; Petrides, 2019) is still widely used, but different approaches for automatic sulcal labelling have been developed (for review, see Mangin et al., 2015b), because manual labelling is complex and sometimes ambiguous, even for trained experts, and it is not sustainable for studying large cohorts. Yet, automatic sulcal labelling is challenging in the fetus and early preterm because of age-related changes in brain size, sulcation, and relative position and size of cortical regions (cf. Fig. 1. C and D and Fig. 5). Hence the development of an automated sulcal labelling for the foetal brain is particularly challenging (cf. Table 2. F).

Group studies further require the images and cortical surfaces to be spatially comparable, which is achieved through *registration* between

subjects. Brains with sufficient anatomical landmarks are compatible with classic MRI registration methods, developed for the adult brain but eventually transposed to the infant, such as atlas-driven registrations using a neonate atlas rather than an adult one (Hill et al., 2010). Yet, when aligning either poorly folded brains or brains at different developmental stages, special care should be taken (cf. Table 2. G). Nevertheless, some methods are compatible or made compatible with the absence of anatomical landmarks, such as the HIP-HOP tool, a 2D sulcal matching approach initially developed for the adult to diffeomorphically register pre-labelled sulci and allow correct alignments of grey and white matter volumes (Auzias et al., 2013). This method does not impose the strict match of specific sulci together but instead optimizes the match between sulci and iso-coordinates in a whole-brain approach, and is therefore compatible with the developing brain, despite its fewer and less developed sulci (Fig. 3. B, Auzias et al., 2015).

As a whole, these refined methods enable precise in-vivo imaging and pre-processing of foetal and neonatal brains and further allow for an increasingly precise investigation of the developing brain, especially in terms of folding.

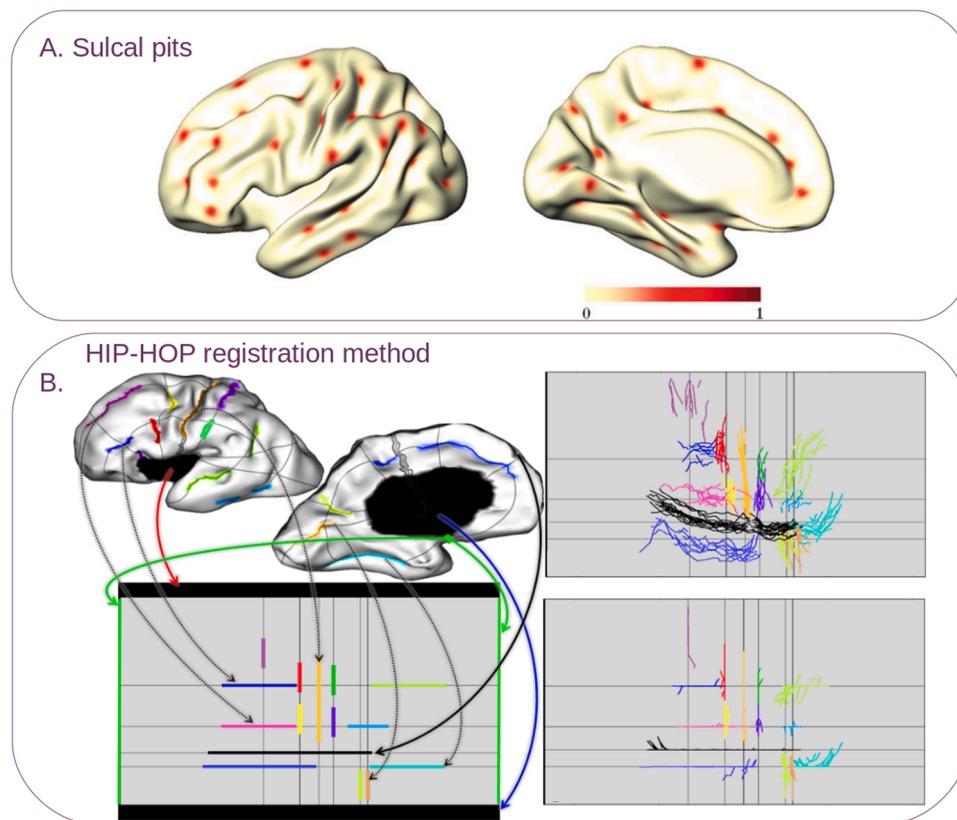


Fig. 3. Illustration of methods based on sulcal considerations. A. Sulcal pits of an individual adult brain projected on an averaged surface template (courtesy of Im et al., 2010). B. Representation of the HIP-HOP method applied to foetal brains. Left. Each sulcus is mapped to a rectangular domain; Top right. Superposition of 15 foetal individuals after unconstrained mapping; Bottom right. Corresponding model with constrained mapping (courtesy of Auzias et al., 2015).

2.2.2. Sulcal analysis methods' adaptation

Sulcal detection methods might allow for the investigation of folding dynamics during development but this requires particular refinements. Global folding approaches developed in the adult can sometimes be transposed to the developing brain. For example, the spectral analysis of gyrification (SPANGY) has been developed to question and quantify the spectral distribution of the global and local shapes of the brain, including the folding patterns (Germanaud et al., 2012). Initially assessed on the adult, it has been applied to the developing brain, leading to a refined comparison of sulcal dynamics between the preterm and term newborn (cf. Fig. 7. B; Dubois et al., 2019). Very much like a Fourier analysis does for temporal signals, the SPANGY tool relies on the spectral decomposition of the cortical surface curvature on a basis of elementary patterns of increasing spatial frequencies, defined at the level of individual brain. This results in the decomposition of folding pattern in 7 spectral bands of increasing frequencies (B0 to B6), in which B0 to B3 bands capture the global shape of the brain while B4, B5, and B6 bands account for the folds shaping with increasing spatial details. By labelling each vertex of the cortical surface according to the locally determinant frequency band, such analysis applied to neonates and infants suggested that B4, B5, and B6 bands match sulci corresponding to primary, secondary and tertiary folding waves that develop non linearly in the preterm and early post-term periods (cf. Fig. 4. B). Another approach, focused on pattern clustering, inferred similarity between multi-view curvature features (decomposed curvature maps at multiple spatial-frequency scales and gyral crest curves) using a similarity network fusion method and a hierarchical affinity propagation clustering approach (Duan et al., 2019). This allowed for folding pattern clustering in the neonate, uncovering representative folding patterns in several brain regions.

In terms of sulcus-specific approaches, in the adult, numerous

methods have been used, to analyse simple metrics (e.g. Pizzagalli et al., 2020), local sulcal index (e.g. Sarrazin et al., 2018), pattern or localization information (e.g. Cachia et al., 2018), or shape features (e.g. Coulon et al., 2015). Some of these metrics are difficult to implement in the developing brain, such as the local sulcal index, for which the sulci are not deep enough to ensure reliable ratios, and others require methodological adaptations. For example, methods which can rely on the stability of the overall sulcal object's size in adults, may need computational adaptation when applied to the developing brain to account for the difference in sulcal size between two time-points during early life (e.g. in the adult: Sun et al., 2016 vs in the preterm infant: de Vareilles et al., 2022).

2.3. Progression of sulcation in the developing human brain

Now that the context of sulcal studies in the developing brain has been set, we aim to detail the progression of sulcation in the human brain, relying on both *post-mortem* and *in-vivo* data obtained in fetuses, in preterm and term-born neonates and in infants, and focusing on the current knowledge about folding dynamics in the developing brain, before 2 years of age. A review on fetal and postnatal development of the cortex addresses cortical folding in a subsection (Dubois and Dehaene-Lambertz, 2015), and a review specifically explores it in the light of sulcal pits (Im and Grant, 2019).

2.3.1. Chronology of the development of folds

Let us first expose the chronology of folds' development. The first observations about the developing folds were made on *post-mortem* foetal specimens. A pioneer study explored 207 serially sectioned brains after excluding brains with obvious malformations, and reported the age of apparition of major fissures and sulci (Chi et al., 1977a). They develop

in three successive folding waves, the primary folds appearing from 20w PMA, the secondary folds from 32w PMA, and the tertiary folds from 38w PMA (Chi et al., 1977a; Feess-Higgins and Laroche, 1987). This question was thereafter reinvestigated using MRI in different populations, including *post-mortem* fetuses (Chi et al., 1977a; Chi, et al., 1977b; Hansen et al., 1993), *in-vivo* fetuses (Garel et al., 2001; Habas et al., 2012), and extremely preterm neonates (Dubois et al., 2008a), in which hemispheric differences in the folds apparition were additionally reported. The results of these different studies are summarized in Table 3 and visualized in Fig. 4. The chronology of folding reported are not strictly the same between studies (we can highlight a lag in the study by Dubois et al., 2008a, which may be due to the minimal depth required to detect a forming sulcus with their methodology, along with partial volume effects present in MRI but not in *post-mortem* visual inspections, and the possibility of damaged or deformed *post-mortem* specimen) yet relay similar trends, which were further confirmed by additional studies not explicitly detailing the chronology of appearance of specific folds, but describing the time-line of sulcation by region.

In addition, the *relative speed of sulcation* has been assessed in the different brain regions (Fig. 5. A; in the fetus: Habas et al., 2012; Wright et al., 2014; in the preterm: Dubois et al., 2008a; Kim et al., 2016b), and these studies reported that the dynamic of sulcation is slower (and linear) in the insula and anterior temporal region compared to the other regions, which show a non-linear folding increase between 20 weeks of gestational age (w GA) and 40w GA (Wright et al., 2014). Sulcation first develops in the area just around the central sulcus and the medial occipital regions, before the parietal, occipital, and posterior temporal regions, which themselves show advances in sulcation compared to the frontal and anterior temporal regions (in the preterm: van der Knaap et al., 1996; Dubois et al., 2008a; in the term-born neonate: Hill et al.,

2010). When comparing growth rates by measuring cortical folding features such as sulcal depth and mean curvature, the ordering of regions is as follows: posterior temporal, parietal, fusiform and parahippocampal, occipital, frontal, temporal medial, and cingulate (in the fetus: Wright et al., 2014; in the preterm: Kim et al., 2016b). As a result, at the age equivalent to full-term birth (~40w GA), all primary and secondary sulci are formed, as well as the majority of tertiary sulci: then the overall sulcal shape is the same in neonates and adults and shows the same folding variability (cf. Fig. 1 B. and C.), with the exception of less convoluted anterior cingulate, anterior temporal cortices, and mid temporal sulcus where a higher sulcal depth variability is observed in neonates than in adults (Hill et al., 2010).

2.3.2. Emergence of folding patterns

In terms of *global folding measures* (by that, we mean non sulcus-specific, including measures such as local gyrification indices), the allometric scaling law between cortical surface area and cerebral volume showed a decreased scaling exponent with decreased gestational age at birth in a preterm population ranging from 22 to 29w GA (Kapellou et al., 2006). Region-wise, the evolution of curvature measures have been reported between 22 and 39w GA in the fetus (Wright et al., 2014), and longitudinally, yet with surprisingly opposite results, in the preterm between 30w and 40w PMA: one study reported the highest gyrification change in the parietal and occipital lobes (Moeskops et al., 2015), while the other one reported that these two regions showed the least increase of folding, and that the highest gyrification change was observed in the prefrontal and temporal lobes (Orasanu et al., 2016). These discordant results are probably due to methodological discrepancies between the two studies, as, for example, region-averaged values were used in Moeskops et al., 2015, which may decrease noise effects

Table 3

Chronology of appearance of sulci according to different studies, ordered by age of appearance in the princeps study Chi et al. (1977a).

Sulcus or fissure	Age of appearance (w GA/PMA)				
	Chi et al. (1977a) <i>post-mortem, visual</i>	Hansen et al. (1993) <i>post-mortem, MRI</i>	Garel et al. (2001) <i>in-vivo, MRI, fetal</i>	Dubois et al. (2008a), <i>in-vivo, preterm, MRI</i> Left/Right	Habas et al. (2012)
Interhemispheric fissure	10	8–13			
Transverse cerebral fissure	10				
Callosal sulcus	14	8–13			
Sylvian fissure	16	8–13			
Calcarine sulcus	16	14–17	22–23		
Olfactory sulcus	16	14–17		32/34	
Parieto-occipital sulcus	16	14–17			
Insula ¹	18				22
Cingulate sulcus	18	14–17	Posterior ² : 22–23 anterior: 22–23		Posterior: 20 anterior: 23
Rhinal sulcus					23
Central sulcus ³	20	18–22	24–25		24
Superior temporal sulcus	23	18–22	Posterior: 26, anterior: 30	27/26.7	25/24
Collateral sulcus	23	18–22	24–25	29/30	24
Uncinate sulcus				30/30	
Precentral sulcus ⁴	24	22–25	26	29/29	27
Postcentral sulcus ⁵	25	22–25	27	28/27	27
Superior frontal sulcus	25	22–25	24–25	30/29	24
Intraparietal sulcus	26	22–25	27	30/29	
Inferior temporal sulcus ⁶	26	22–25	30	30/29	
Occipital sulcus	27	22–25			
Inferior frontal sulcus	28	26–29	26	30/30	
Occipito-temporal sulcus ⁷	30	26–29	29		
Secondary cingular sulci*	32		31		
Secondary occipital sulci*	34		32		
Insular sulci*	34–35		33		

Some sulci are given different names. We adopted the nomenclature from section 1.1, but the other possible names are the following: 1: Circular sulcus, 2: Marginal sulcus, 3: Rolandic sulcus, 4: Prerolandic sulcus, 5: Postrolandic sulcus, 6: middle temporal sulcus, 7: inferior temporal sulcus. *groups of sulci preventing us from using matching nomenclature

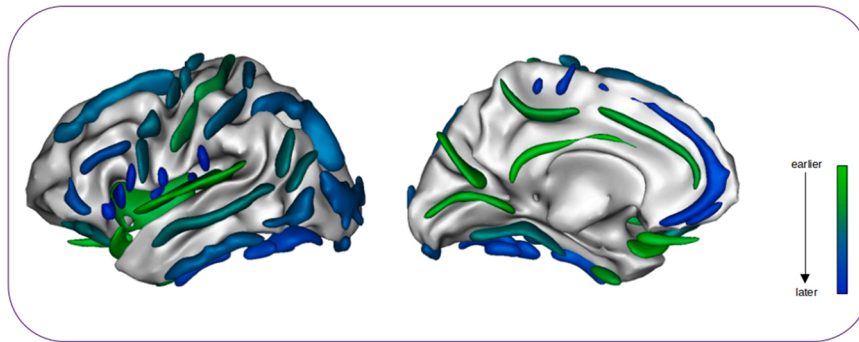


Fig. 4. Chronology of the apparition of folds illustrated on a left hemisphere (lateral and medial views), corresponding to ages reported in Table 3. The main sulci range from early (green) to late (deep blue) development as detailed in the reference article Chi et al. (1977a).

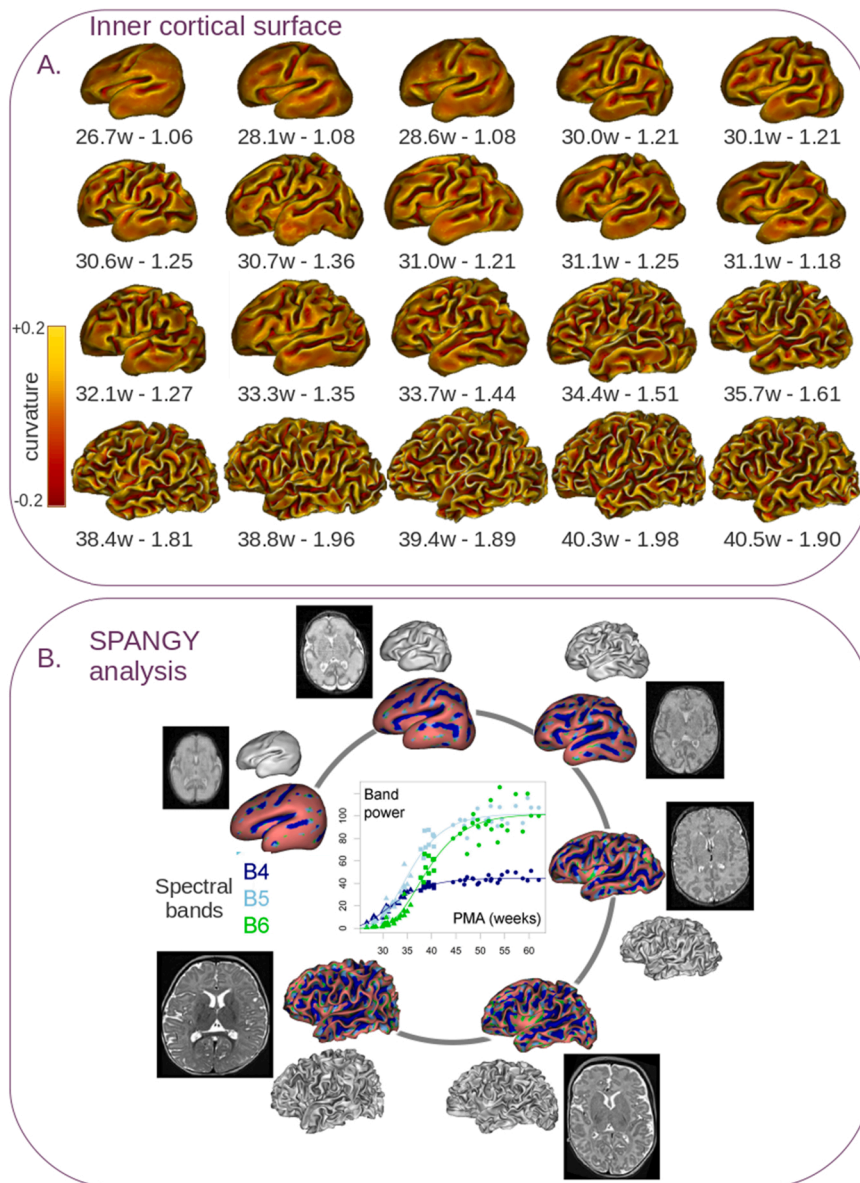


Fig. 5. Evolution of cortical folding in the human brain (Courtesy of Dubois et al., 2019). A. Reconstructions of inner cortical surface of preterm newborns of different post-menstrual ages (left number) and whole-brain sulcation index (right number). The colours outline the surface curvature. The surfaces are displayed with the same spatial scale. B. Illustration of the evolution of folding based on SPANGY analysis and plots of spectral band power as a function of post-menstrual age (B4, B5 and B6 can be considered as proxies of primary, secondary and tertiary folding respectively).

against a loss in precision.

After normal-term birth, sulcation was reported to evolve differently between 0 and 1 year and 1–2 years of age, with *sulcation rates decreasing with development* (Li et al., 2014) and sulcal complexity increasing

between 6 months and 2 years of age (Kim et al., 2016a). Even though the different cortical regions show asynchronous sulcal growth, the global stability of the folding patterns between birth and 2 years of age has been assessed using sulcal pits, whose location and concentration

were kept almost unchanged (Meng et al., 2014). Moreover, a study assessed whether brains which looked alike at birth evolved similarly at 1 year of age, and obtained relevant correlations (Rekik et al., 2018), suggesting that dynamic consistency of folding pattern is extendable to inter-subject considerations.

On a more *sulcus-focused approach*, some studies reported specific measures on a number of sulci, either in a longitudinal setting in preterm infants, reporting the relative growth of sulci in terms of length and surface area between 30 and 40w PMA (Kersbergen et al., 2016), or in the assessment of fetuses ranging from 20 to 28w GA, reporting the evolution of mean curvature (Habas et al., 2012). These studies have given valuable overview of sulcation on the whole-brain-scale. More pattern-oriented studies on the former preterm cohort reported an important conservation of pattern both in the central sulcus (de Vareilles et al., 2022) and in the Sylvian fissure (De Vareilles et al., 2023), suggesting an early encoding of the shape specificities of these two primary folds from 30w PMA. Using a multi-age fetal atlas, a study focusing on the links between genetics and opercularization precisely characterized the growth dynamics around the insula through Jacobian vector fields in fetuses between 21 and 38w GA, showing the volumetric expansion of the frontal, temporal and parietal opercula throughout this developmental period (Mallela et al., 2020).

These folding processes, which concur with other developmental mechanisms, could be important in the development of functional specialization, seeing that sulcal anatomo-functional correlates are observed in the adult (Jiang et al., 2021).

3. Functional relevance of early sulcal development

Studies linking early cortical folding and functional development are scarce. Yet, since sulcal patterns emerging before the age of one year have been linked to cognitive (e.g. Cachia et al., 2018), functional (e.g. Sun et al., 2016) and pathological outcomes (e.g. Gay et al., 2017) at later ages, it seems that essential information is encoded at a young age. Before novel studies reach to investigate this subject further, the functional relevance of cortical folding specificities is here questioned with the lens of functional lateralization and deviations from the typical developmental trajectory.

3.1. Early asymmetries in folding across hemispheres

Functional lateralization is a major characteristic of the human brain, in particular regarding the language, sensorimotor and face processing networks that develop early on to sustain the behavioural acquisitions of infants (Dehaene-Lambertz and Spelke, 2015). The extent to which the emergence of this lateralization is based on early anatomical substrates during development has come to the fore in recent years, leading to recent studies on inter-hemispheric asymmetries. Findings suggest a general functional dominance of the right hemisphere except for linguistic stimuli, as well as an earlier overall development of the right hemisphere compared to the left one (Bisiacchi and Cainelli, 2022). One of the developmental mechanisms studied in terms of asymmetries is the brain folding as several correlations in the adult brain have been demonstrated between functional lateralization and asymmetries in sulcation (e.g. Sun et al., 2016; Tissier et al., 2018), suggesting anatomo-functional relationships in asymmetrical sulci. In terms of hemisphere-wise development, the right hemisphere shows folding onset and sulcal complexity earlier than the left one (Chi et al., 1977a; Dubois et al., 2008a; Habas et al., 2012). This *sulcation asynchrony across brain hemispheres* is the most striking developmental asymmetry. Yet, the left hemisphere globally catches up to the right one later on. This approximate 2-week lag may explain the increased inter-individual variability observed in the right hemisphere between 27 and 36w PMA (Dubois et al., 2010). Conversely, the left hemisphere has recently been reported to show advance in opercularization, which could explain the lasting length asymmetry of the Sylvian fissure (De Vareilles et al.,

2023) and suggests fundamentally different dynamics in opercularization versus sulcation.

During the perinatal period, two sulcal asymmetries are most consistently reported: the left *Sylvian Fissure* is longer and less curved than the right one (Fig. 6. A; post-mortem: Chi et al., 1977a; in the fetus: Habas et al., 2012; in the preterm: Dubois et al., 2010; Kersbergen et al., 2016; in the term-born neonate: Hill et al., 2010; Glasel et al., 2011), and the right *superior temporal sulcus* – more specifically its medium part – is deeper in the right hemisphere (Fig. 6. B; in the fetus: Habas et al., 2012; in the preterm: Dubois et al., 2008a; Dubois et al., 2010; Kersbergen et al., 2016; in the term-born neonate: Hill et al., 2010; Glasel et al., 2011; Li et al., 2014; Bozek et al., 2018). Interestingly, Glasel et al., 2011 reported an absence of correlation between the rightward superior temporal sulcus and leftward Sylvian fissure asymmetries, which supports the idea of a difference in morphogenetic processes inducing both phenomena (i.e. sulcation on one hand versus opercularization on the other hand). These early asymmetries may be related to the *early functional specialization for language perception and processing*, which is reported to be asymmetrically observed as soon as birth in the planum temporale (Dehaene-Lambertz et al., 2006).

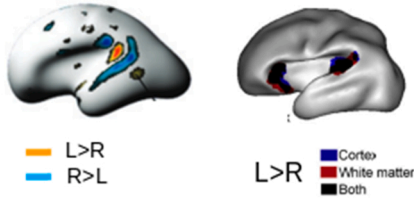
Additional sulcal asymmetries during development have been reported using classical length and depth measures. In terms of rightward asymmetries, we can name the dorsolateral portion of the right central sulcus, as soon as 27w GA (Fig. 6. C; in the fetus: Habas et al., 2012; in the term-born neonate: Li et al., 2014), the insula in the preterm infant at term-equivalent age (TEA) (in terms of surface rather than depth; Kersbergen et al., 2016), the inferior frontal sulcus at 30w PMA and TEA in the preterm infant (Kersbergen et al., 2016), and the lateral occipito-temporal sulcus in term-born neonates (Bozek et al., 2018). In terms of leftward asymmetries, we can mention the parieto-occipital sulcus at 26w GA in the fetus (Habas et al., 2012), and the anterior part of the temporal lobe, both medial and lateral, in the term born infant (Bozek et al., 2018). The superior frontal sulcus has been reported to show a reversed asymmetry with age, being deeper in the left hemisphere at 27w GA (Habas et al., 2012) but deeper in the right hemisphere at 40w PMA (Kersbergen et al., 2016).

Finer asymmetries can be captured by looking further into *shape and pattern*. When focusing on sulcal length, the descriptions for the Sylvian fissure are limited to a longer left Sylvian fissure (Chi, . et al., 1977b), while a voxel-based analysis better characterized that it extends more anteriorly and posteriorly than the right fissure (Dubois et al., 2010), and a sulcal shape analysis additionally reported that left fissures tend to be flatter and to branch more than their right counterparts both at 30w PMA and TEA, and that the left supramarginal gyrus tends to be more profoundly anchored in the Sylvian fissure than the right at TEA (Fig. 6. A; De Vareilles et al., 2023). Looking into the localization of sulcal pits, hemispheric differences have also been revealed in the neonate: the superior temporal sulcus showed more anterior pits in the right temporal pole; the superior part of the postcentral sulcus showed a sulcal pit cluster on the left but not on the right side; and the left central sulcus' pits were more dorsal than its right counterpart (Meng et al., 2014). This central sulcus asymmetry can be paralleled with the asymmetry previously reported in the adult brain (Sun et al., 2012), and newly reported in the preterm infant at TEA (Fig. 6. C; de Vareilles et al., 2022): the single to double-knob configuration, with right central sulci preferring the single-knob configuration, and the left ones favouring the double-knob configuration. In the adult, this specific asymmetry was related to handedness, with significant differences in single-to-double-knob configurations in left-handers compared to right-handers (Sun et al., 2012). The observation of a similarly asymmetrical shape feature in the neonate raises questions about potentially early functional specialization regarding handedness. This last study (de Vareilles et al., 2022) additionally reported a hand-knob depth asymmetry at 30w PMA, while a previous study capturing only length and surface area failed to capture an asymmetry at 30w PMA (Kersbergen et al., 2016), highlighting the additional information gained through

A. Sylvian fissure

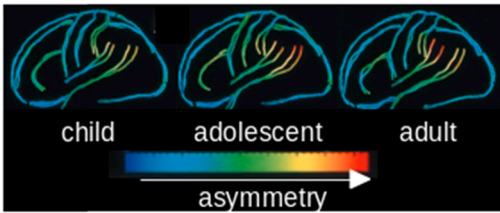
1. Whole-brain analyses

Fetus, 27w GA Curvature analysis Preterm, 27-36w PMA Voxel-based analysis

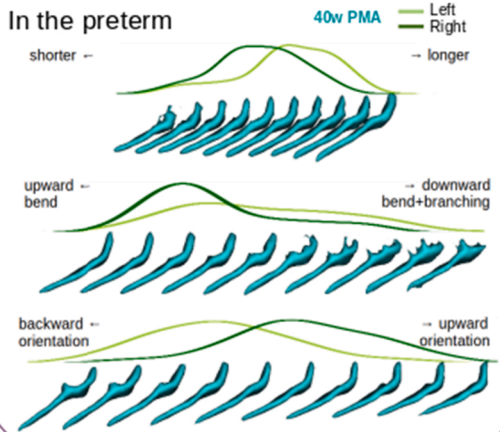


2. Sulcus-specific studies

From childhood to adulthood



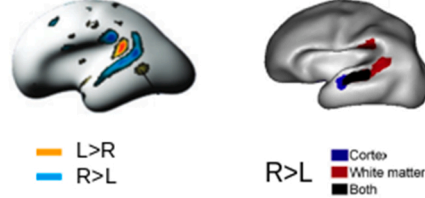
In the preterm



B. Superior temporal sulcus

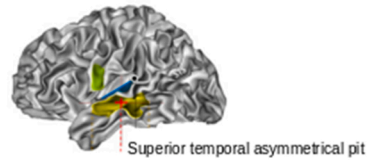
1. Whole-brain analyses

Fetus, 27w GA Curvature analysis Preterm, 27-36w PMA Voxel-based analysis

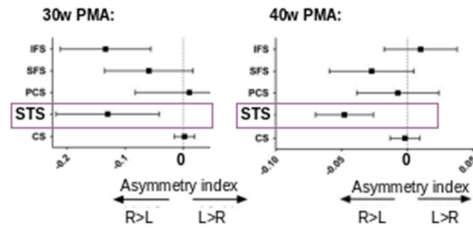


2. Sulcus-specific studies

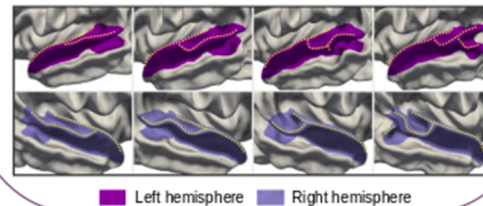
In the child and in the adult



In the preterm



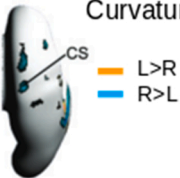
At term



C. Central sulcus

1. Whole-brain analyses

Fetus, 27w GA Curvature analysis

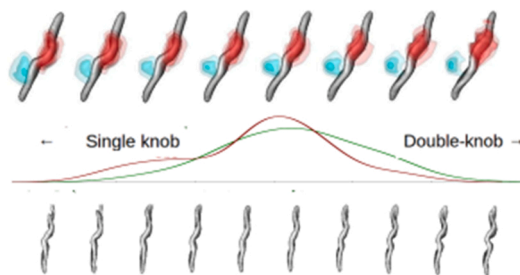


2. Sulcus-specific studies

In the adult
 Hand activation (red)
 Silent reading (blue)

At 40w PMA

Left (green)
 Right (red)



(caption on next page)

Fig. 6. Main sulcal asymmetries in the developing brain. **A. Sylvian fissure.** 1. Curvature asymmetries are reported in the fetus at 27w GA comprising the posterior end of the Sylvian fissure (courtesy of Habas et al., 2012), and grey and white matter leftward volume asymmetries in the preterm between 27 and 36w PMA (courtesy of Dubois et al., 2010). 2. Sulcal asymmetries are captured from childhood to adulthood and increase with age (courtesy of Sowell et al., 2002); in the preterm, asymmetric shape features have been captured at 30 and 40w PMA (representation of 40w PMA shape features with asymmetrical distributions; courtesy of De Vareilles et al., 2023). **B. Superior temporal sulcus.** 1. Curvature asymmetries are reported in the fetus at 27w GA comprising the superior temporal sulcus (courtesy of Habas et al., 2012), and grey and white matter rightward volume asymmetries in the preterm between 27 and 36w PMA (courtesy of Dubois et al., 2008a). 2. In the child and the adult, an asymmetry is captured in the Superior Temporal Asymmetrical Pit (courtesy of Leroy et al., 2015); in the preterm, rightwards surface asymmetries have been reported at 30 and 40w PMA (courtesy of Kersbergen et al., 2016); at term, asymmetrical gyral patterns have been reported in the superior temporal gyrus (courtesy of Duan et al., 2019). **C. Central sulcus.** 1. Limited curvature asymmetry is reported in its superior extremity at 27w GA in the fetus (courtesy of Habas et al., 2012). 2. In the adult, asymmetrical shape feature captured (Sun et al., 2012) and associated with localization of functional activations (hand activation and silent reading on the left central sulcus; image courtesy of Sun et al., 2016); at term-equivalent age in the preterm, a similar shape feature is captured, with a right hemisphere tendency towards a single-knob configuration and a left hemisphere tendency towards a double-knob configuration (courtesy of de Vareilles et al., 2022). w GA: weeks of gestational age; w PMA: weeks of post-menstrual age; L: left; R: right; STS: superior temporal sulcus; CS: central sulcus.

shape characterization. In a mix of TEA preterm and term-born neonates, pattern-specific asymmetries have also been reported in the superior temporal gyrus and in the cingulate cortex, in which some pattern occurrences seem to develop only in a given hemisphere (Fig. 6. B; Duan et al., 2019).

3.2. Early deviations in cortical folding

Another aspect suggesting the functional relevance of the early folding process is that its trajectory might be altered early on by some pre- or post-natal perturbations and in relation with later functional consequences. Even though we have presented jointly results of cortical folding observed in the fetus, in the premature infant, and in the term-born infant, it should be noted that *some clinical conditions lead to*

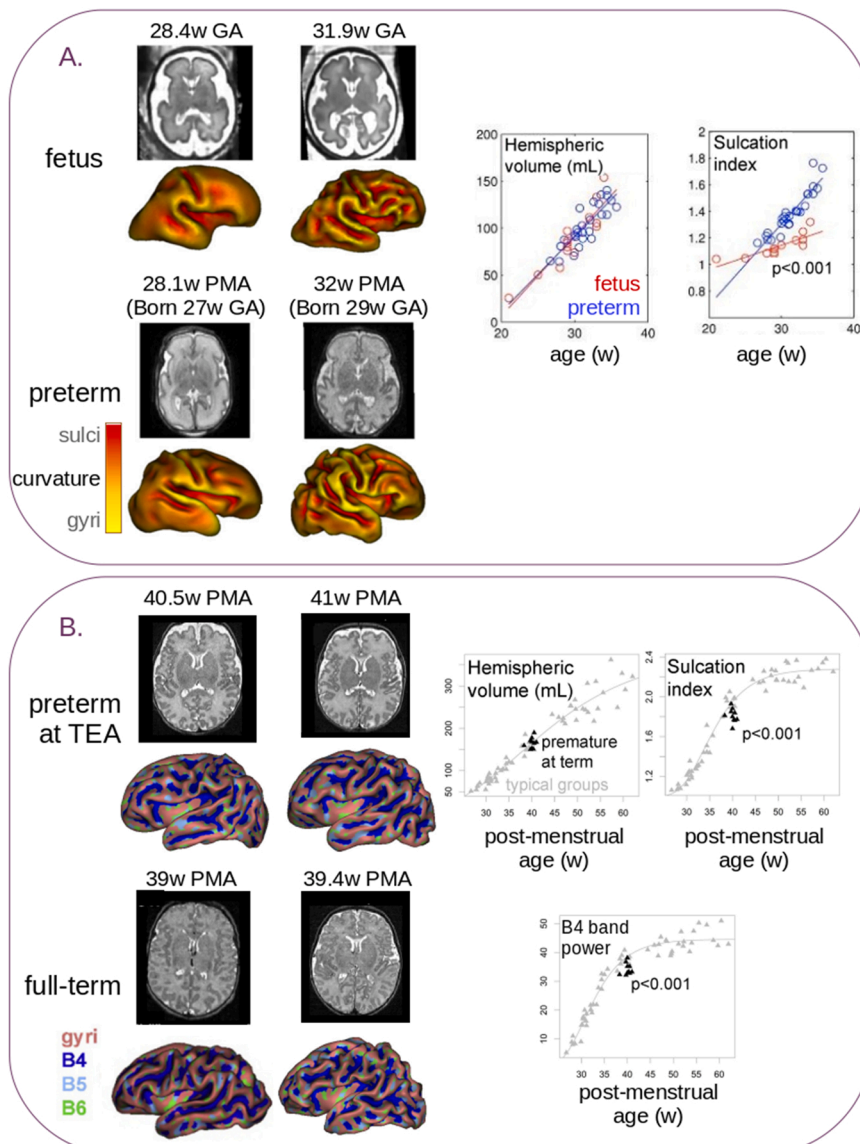


Fig. 7. Comparisons between preterm and typical populations. **A. Left:** Representation of axial MRI slice and corresponding volumetric reconstructions of cortical meshes at multiple ages in the typically developing fetus (top rows) and in the preterm (bottom rows). The colours outline the surface curvature. **Right:** graphs of hemispheric volumes and sulcation index (red: fetuses, blue: preterm infants; courtesy of Lefèvre et al., 2016). **B. Left:** Representation of axial MRI slice and corresponding volumetric reconstructions of cortical meshes at multiple ages in the preterm at term-equivalent age (top rows) and in the term-born neonate (bottom rows). The colours outline the gyri and SPANGY spectral bands. **Right:** graphs of hemispheric volumes, sulcation index, and B4 band power (black: preterm at term-equivalent age, grey: typical populations; courtesy of Dubois et al., 2019).

folding alterations, even in the case of non-pathological situations. Without addressing pathologies of sulcation, such as lissencephaly or polymicrogyria (addressed in Massimo and Long, 2022), some conditions should be mentioned: as a non-pathological example, being a twin was associated with a delay in folding dynamics (Chi et al., 1977a; Dubois et al., 2008b). In pathological circumstance, both pathologies with important anatomical brain alterations (such as agenesis of the corpus callosum; Tarui et al., 2018, or ventriculomegaly; Benkarim et al., 2018) or with genetic origins (such as Down's syndrome; Yun et al., 2021) have been reported to influence sulcation in the fetus. In terms of onset of folding alterations, by comparing early images of fetuses which would show abnormal folding pattern after birth with control fetuses, it was reported that while showing normal gyrification indices at early scan, the subjects which would present folding anomalies already significantly differed from templates, mostly in terms of location and depth pattern of sulcal basins, indicating early onset of sulcal pattern deviations (Im et al., 2017).

In preterm infants, in addition to the environmental difference between *in-utero* and *ex-utero* brain development (Fig. 7. A; Lefevre et al., 2016), extreme *prematurity* is often associated with clinical disturbances which may affect normal brain development, including sulcal appearance, such as gestational age at birth, multiple pregnancies, intra-uterine growth restriction (IUGR), early-life severe illness indicators (such as necessity for prolonged mechanical ventilation, exposure to critical illness in the first 24 h of life, and early exposure to steroids), and presence of brain injuries. Gestational age at birth was shown to impact sulcal development in preterm infants, with decreasing divergence from control fetal development with increasing gestational age at birth (Fig. 7A; Lefevre et al., 2016). In extremely preterm populations, being part of a multiple pregnancy led to a delayed but harmonious maturation (Dubois et al., 2008b; Kersbergen et al., 2016). IUGR, either reported as such, as low birth-weight according to GA, or as smaller head circumference at birth, was linked to a discordant folding trajectory, either through disproportionate alterations in sulcation index compared to a decreased surface and volumetric growth (Dubois et al., 2008b), or through lower gyrification index and cortical surface area (Engelhardt et al., 2015), but also through decreased Sylvian fissure and insula surface area at 30w PMA, and smaller left insula, left superior temporal sulcus, and bilateral central sulcus at TEA (Kersbergen et al., 2016).

In terms of early-life severe illness indicators, higher critical illness in the first 24 h, exposure to postnatal steroids, and to prolonged mechanical ventilation were related to decreased cortical surface area in infants (Engelhardt et al., 2015). Prolonged mechanical ventilation was linked to reduced surface area of the insula and Sylvian fissure as well as to reduced depth in the right central sulcus at 30w PMA, and to a smaller right superior temporal sulcus and a shallower left precentral sulcus at TEA (Kersbergen et al., 2016). Finally, different types of brain injuries were reported in links to altered sulcation. Extremely preterm infants with cortical grey matter anomalies showed increased cortical thickness and decreased cortical folding at TEA, which was more pronounced than at 30w PMA (Moeskops et al., 2015). This concurs with the observation that preterm infants with brain injury can be differentiated from those without (Shimony et al., 2016). Severe intraventricular haemorrhage (IVH) was reported to only be associated with a reduced presence of secondary sulci at 30w PMA (Kersbergen et al., 2016), in agreement with another study which linked IVH, periventricular leukomalacia, and ventriculomegaly to reduced cortical folding before 31w PMA but not later (Kim et al., 2020). In this same study (Kim et al., 2020), at term-equivalent age, no difference was found in cortical folding captured through sulcal depth between these subjects and both non-injured preterm and term-born infants, but they showed altered organization of cortical folds.

More generally, altered sulcation has been reported in premature infants and children. Prematurity per se seems to be a motive of altered sulcal dynamics because of the difference between *in-utero* and *ex-utero* environment during sulcal development. When compared to same-age

fetuses, the preterm brain without any obvious brain anomaly still shows less cerebrospinal fluid, more pronounced folds, and a more compact global shape (Fig. 7A; Lefevre et al., 2016). This study additionally reported that preterm birth is linked to an increase in intensity and sharpness of folding, as well as altered sulcal shape, and this observation was modulated by GA at birth.

Compared to moderate preterm newborns, extremely premature infants showed reduced cortical growth in a number of different regions (namely: the superior frontal, occipital, basal temporal, precuneus, right superior and middle temporal and parahippocampal gyri as well as the right central sulcus area; Kim et al., 2016b). Yet, this study design did not allow the authors to differentiate direct effects of prematurity on sulcation from indirect effects linked to adversarial situations linked to prematurity, as it did not exclude preterm subjects with brain injuries or clinical factors susceptible to alter cortical development. Additionally, the regions reported did not overlap with those observed in an alternative study set-up, comparing extremely preterm infants – selected to exclude periventricular leukomalacia, intra-ventricular haemorrhage of grade III and IV, focal brain lesions and persistent ventricular dilatation at TEA – with term-born controls: this study reported reduced grey matter in the bilateral temporal lobes, pre and post-central gyri, orbitofrontal cortex, amygdala, para-hippocampal gyrus, hippocampus and left insula (Padilla et al., 2015). Finally, when compared with term-born neonates, extremely preterm infants at TEA showed a less complex gyrification (captured through the whole-cortex convolution index: Ajayi-Obe et al., 2000; the gyrification index: Engelhardt et al., 2015; Shimony et al., 2016; the folding power corresponding to different spectral bands: Dubois et al., 2019; Fig. 7B). A specific impact on the insula, superior temporal sulcus, and ventral pre- and postcentral sulci was also reported (Engelhardt et al., 2015), compatible with the observation that the B4 spectral band, most likely corresponding to primary sulci wave, showed the most significant decrease in TEA preterm infants compared to term-born infants, suggesting that sulci developing during the period of preterm birth are most impacted, while later-developing sulci are still impacted but less (Dubois et al., 2019). When comparing adults who were born very preterm to aged-matched control adults, alterations in folding of the frontal, temporal, parietal, and occipital regions were reported (either through an increase of absolute mean curvature: Hedderich et al., 2019; or through a decrease in local gyrification index: Papini et al., 2020). In both cases, more important deviations from control adults were associated with lower IQ scores, suggesting intertwining between sulcation and cognitive development.

3.3. Relation to functional development in the preterm infant

Reading the adult studies showing relationships between functional activations and folding and the infant studies describing early alterations in folding patterns suggests that this anatomical characteristic might also convey some functional information during development. To the best of our knowledge, the only studies assessing the relationship between early cortical folding and later functional outcome have been conducted on preterm infants (Kapellou et al., 2006; Dubois et al., 2008b; Kersbergen et al., 2016; de Vareilles et al., 2022). While these studies do not allow us to differentiate typical folding dynamics from prematurity-induced ones, they are currently the only access we have to correlations between sulcal shape and later functional outcome. The two former studies (Kapellou et al., 2006; Dubois et al., 2008b) have assessed global folding metrics and their link to later cognitive development, either at 2 years of age using Griffiths Mental Development Scales: Revised 1996 (Kapellou et al., 2006) or at term-equivalent age using the Assessment of Preterm Infant's Behaviour (APIB) (Dubois et al., 2008b). Both reported a link between a decreased cortical surface area at birth and lower cognitive scores.

The two latter studies (Kersbergen et al., 2016; de Vareilles et al., 2022) have focused on specific sulci in a cohort of longitudinally

scanned preterm infants at 30 and 40w PMA. Using surface area, mean depth and sulcation index as sulcal measures, as well as their increase between the two assessments, significant associations were found between a number of sulci and motor, cognitive and language scores assessed at 2 or 2.5 years of age with the Bayley Scales of Infant and Toddler Development, third edition (BSID-III), through the use of a general linear model (Kersbergen et al., 2016). More precisely, for motor outcome, at 30w PMA, relationships were reported for gross motor outcome and the inferior frontal sulcus (in terms of surface area, depth and sulcal index) and the right superior frontal sulcus (depth). For fine motor outcome, effects were reported at 40w PMA for the right post-central sulcus (surface area) and the right superior temporal sulcus (depth). For cognition, relationships were observed for the depth increase of the left Sylvian fissure and superior frontal sulcus between both ages. In terms of language outcome, at 30w PMA, effects were reported for the left inferior frontal sulcus (surface area and sulcal index for receptive scores, surface area only for expressive scores). At 40w PMA, effects were reported for receptive scores in the Sylvian fissure (surface area, depth and sulcal index in both hemispheres), the superior temporal sulcus (right surface area and sulcal index, depth in both hemispheres), the left insula (surface area and sulcal index), and the inferior frontal sulcus (depth in both hemispheres), while only the left Sylvian fissure (depth) showed an effect on expressive language outcome.

The absence of relationships observed between basic measures in the central sulcus and motor outcome led another study to question the relevance of sulcal pattern to predict later motor outcome (de Vareilles et al., 2022). After quantifying the main shape features for the central sulci of the preterm cohort at both ages (as detailed in the methods section, part c.), the shape features of either the left or right hemisphere, at either 30 or 40w PMA, were used as an input for a support vector classifier, to predict motor development assessed at around 5 years of age, either in terms of manual laterality (left or right handedness) on one hand, or normal and pathological fine motor outcome using the Movement Assessment Battery for Children, 2nd edition (MABC-2) on the other hand. Even though none of the resulting classifiers demonstrated significant predictive capacity, some showed a trend towards significance and most performed better than a baseline classifier trained using clinical factors which were previously indicated as important for prediction of motor outcome (Anderson and Doyle, 2006; Kersbergen et al., 2016). These classifiers suggested that sulcal pattern of the central sulcus at 30w PMA on the left hemisphere was the most relevant for predicting handedness and that both left sulcus at 30w PMA and right sulcus at 40w PMA were most relevant for predicting adversarial fine motor outcome, and visual indications about sulcal pattern features linked to the different outcomes were subsequently inferred.

4. Conclusion

More studies should focus on the early folding of the brain and its consequences, including functional relevance of early folding pattern in term-born infants. The first sulco-functional studies being focused on premature cohorts, such studies of typical development would inform both on the normal progression and inter-individual variability, and on the sulcation divergences incurred by prematurity. Moreover, should longitudinal studies be carried on longer periods, assessing sulcal evolution before, at and long after birth, we could get a better understanding of the broader sulcal development process, as even though the most striking folding changes occur before two years of age, we cannot consider the two-year-old brain as mature. Additionally, sulcal studies should be undertaken and reproduced on bigger cohorts, which is starting to be possible thanks to current trends and advances in open data, including the acquisition and sharing of valuable datasets (e.g. for the neonatal brain: the developing Human Connectome Project, <http://www.developingconnectome.org/>), and the incentive to publish experimental processes and codes.

It is essential to carry on the recent efforts made in multi-modal

sulcal considerations. Because of our yet limited understanding of the ins and outs of sulcation, it seems crucial to assess the relationship between different but intertwined concepts, such as for example the maturation of microstructure in relation to the development of sulci (e.g. for cortical microstructure: Wang et al., 2017; Leberberg et al., 2019; Dubois, 2021). Similarly, combining functional and anatomical imaging has already proven to be relevant in the adult (e.g. Sun et al., 2016; Germann et al., 2019) and should be assessed in the neonate. Genetic imaging combined to anatomical MRI (e.g. Mallela et al., 2020; Vasung et al., 2021) is also a promising topic to better understand the fundamentals of cortical folding. Recent studies have paved the way for the assessment of these considerations, and the increased efforts in sulcal studies bode well for the future comprehension of the folding of the brain.

Funding

The project was supported by the IdEx Université Paris (ANR-18-IDEX-0001), the Mésidite Foundation (grant 2018-00092867), the Fondation de France (grant 2020-00111908), the FRM (grant DIC20161236445), the ANR (ANR-14-CE30-0014-02 APEX, grants ANR-19-CE45-0022-01 IFOPASUBA, ANR-20-CHIA-0027-01 FOLD-DICO, ANR-20-CE17-0014-03) and the European Union's Horizon 2020 Research and Innovation Programme through Grant Agreement No. 785907 & 945539 (HBP SGA2 & SGA3).

Declaration of Competing Interest

The authors declare that they have no known competing financial interests or personal relationships that could have appeared to influence the work reported in this paper.

References

- Adamson, C.L., Alexander, B., Ball, G., Beare, R., Cheong, J.L.Y., Spittle, A.J., Doyle, L.W., Anderson, P.J., Seal, M.L., Thompson, D.K., 2020. Parcellation of the neonatal cortex using surface-based Melbourne children's regional infant brain atlases (M-CRIB-S). *Sci. Rep.* 10, 4359. <https://doi.org/10.1038/s41598-020-61326-2>.
- Ajayi-Obe, M., Saeed, N., Cowan, F., Rutherford, M., Edwards, A., 2000. Reduced development of cerebral cortex in extremely preterm infants. *Lancet* 356, 1162–1163. [https://doi.org/10.1016/S0140-6736\(00\)02761-6](https://doi.org/10.1016/S0140-6736(00)02761-6).
- Aleman-Gomez, Y., Janssen, J., Schnack, H., Balaban, E., Pina-Camacho, L., Alfaro-Almagro, F., Castro-Fornieles, J., Otero, S., Baeza, I., Moreno, D., Bargallo, N., Parellada, M., Arango, C., Desco, M., 2013. The human cerebral cortex flattens during adolescence. *J. Neurosci.* 33, 15004–15010. <https://doi.org/10.1523/JNEUROSCI.1459-13.2013>.
- Anbeek, P., Išgum, I., van Kooij, B.J.M., Mol, C.P., Kersbergen, K.J., Groenendaal, F., Viergever, M.A., de Vries, L.S., Benders, M.J.N.L., 2013. Automatic segmentation of eight tissue classes in neonatal brain MRI. *PLoS ONE* 8, e81895. <https://doi.org/10.1371/journal.pone.0081895>.
- Anderson, P.J., Doyle, L.W., 2006. Neurodevelopmental outcome of bronchopulmonary dysplasia. *Semin. Perinatol.* 30, 227–232. <https://doi.org/10.1053/j.semperi.2006.05.010>.
- Auzias, G., Lefevre, J., Le Troter, A., Fischer, C., Perrot, M., Regis, J., Coulon, O., 2013. Model-driven harmonic parameterization of the cortical surface: HIP-HOP. *IEEE Trans. Med. Imaging* 32, 873–887. <https://doi.org/10.1109/TMI.2013.2241651>.
- Auzias, G., De Guio, F., Pepe, A., Rousseau, F., Mangin, J.-F., Girard, N., Lefevre, J., Coulon, O., 2015. Model-driven parameterization of fetal cortical surfaces, in: 2015 IEEE 12th International Symposium on Biomedical Imaging (ISBI). Presented at the 2015 IEEE 12th International Symposium on Biomedical Imaging (ISBI 2015), IEEE, Brooklyn, NY, USA, pp. 1260–1263. <https://doi.org/10.1109/ISBI.2015.7164103>.
- Bae, I., Chae, J.-H., Han, Y., 2021. A brain extraction algorithm for infant T2 weighted magnetic resonance images based on fuzzy c-means thresholding. *Sci. Rep.* 11, 23347. <https://doi.org/10.1038/s41598-021-02722-0>.
- Bartley, A., Jones, D., Weinberger, D., 1997. Genetic variability of human brain size and cortical gyral patterns. *Brain* 120, 257–269. <https://doi.org/10.1093/brain/120.2.257>.
- Bayly, P.V., Taber, L.A., Kroenke, C.D., 2014. Mechanical forces in cerebral cortical folding: a review of measurements and models. *J. Mech. Behav. Biomed. Mater.* 29, 568–581. <https://doi.org/10.1016/j.jmbm.2013.02.018>.
- Benkarim, O.M., Hahner, N., Piella, G., Gratacos, E., González Ballester, M.A., Eixarch, E., Sanroma, G., 2018. Cortical folding alterations in fetuses with isolated non-severe ventriculomegaly. *NeuroImage: Clin.* 18, 103–114. <https://doi.org/10.1016/j.nicl.2018.01.006>.

- Bisiacchi, P., Cainelli, E., 2022. Structural and functional brain asymmetries in the early phases of life: a scoping review. *Brain Struct. Funct.* 227, 479–496. <https://doi.org/10.1007/s00429-021-02256-1>.
- Blanton, R.E., Levitt, J.G., Thompson, P.M., Narr, K.L., Capetillo-Cunliffe, L., Nobel, A., Singerman, J.D., McCracken, J.T., Toga, A.W., 2001. Mapping cortical asymmetry and complexity patterns in normal children. *Psychiatry Res.: Neuroimaging* 107, 29–43. [https://doi.org/10.1016/S0925-4927\(01\)00091-9](https://doi.org/10.1016/S0925-4927(01)00091-9).
- Borne, L., 2019. Design of a top-down computer vision algorithm dedicated to the recognition of cortical sulci. PhD thesis, Université Paris-Saclay.
- Borrell, V., 2018. How cells fold the cerebral cortex. *J. Neurosci.* 38, 776–783. <https://doi.org/10.1523/JNEUROSCI.1106-17.2017>.
- Boucher, M., Whitesides, S., Evans, A., 2009. Depth potential function for folding pattern representation, registration and analysis. *Med. Image Anal.* 13, 203–214. <https://doi.org/10.1016/j.media.2008.09.001>.
- Bouyeure, A., Dubois, J., Germanaud, D., Leroy, F., Mangin, J.F., Lefevre, J., de Vries, L., Groenendal, F., Chiron, C., Hertz-Pannier, L., Benders, M., Noulhiane, M., 2017. Sulcal morphology in the medial temporal lobe in healthy preterm infants. Organization for Human Brain Mapping Meeting (OHBM 2017), Vancouver, Canada.
- Bozek, J., Makropoulos, A., Schuh, A., Fitzgibbon, S., Wright, R., Glasser, M.F., Coalson, T.S., O'Muircheartaigh, J., Hutter, J., Price, A.N., Cordero-Grande, L., Teixeira, R.P.A.G., Hughes, E., Tumor, N., Baruteau, K.P., Rutherford, M.A., Edwards, A.D., Hajnal, J.V., Smith, S.M., Rueckert, D., Jenkinson, M., Robinson, E. C., 2018. Construction of a neonatal cortical surface atlas using multimodal surface matching in the developing human connectome project. *NeuroImage* 179, 11–29. <https://doi.org/10.1016/j.neuroimage.2018.06.018>.
- Cachia, A., Mangin, J.-F., Riviere, D., Kherif, F., Boddaert, N., Andrade, A., Papadopoulos-Orfanos, D., Poline, J.-B., Bloch, I., Zilbovicius, M., Sonigo, P., Brunelle, F., Regis, J., 2003. A primal sketch of the cortex mean curvature: a morphogenesis based approach to study the variability of the folding patterns. *IEEE Trans. Med. Imaging* 22, 754–765. <https://doi.org/10.1109/TMI.2003.814781>.
- Cachia, A., Borst, G., Tissier, C., Fisher, C., Plaze, M., Gay, O., Riviere, D., Gogtay, N., Giedd, J., Mangin, J.-F., Houde, O., Raznahan, A., 2016. Longitudinal stability of the folding pattern of the anterior cingulate cortex during development. *Dev. Cogn. Neurosci.* 19, 122–127. <https://doi.org/10.1016/j.dcn.2016.02.011>.
- Cachia, A., Roell, M., Mangin, J.-F., Sun, Z.Y., Jobert, A., Braga, L., Houde, O., Dehaene, S., Borst, G., 2018. How interindividual differences in brain anatomy shape reading accuracy. *Brain Struct. Funct.* 223, 701–712. <https://doi.org/10.1007/s00429-017-1516-x>.
- Cachia, A., Borst, G., Jardri, R., Raznahan, A., Murray, G.K., Mangin, J.-F., Plaze, M., 2021. Towards deciphering the foetal foundation of normal cognition and cognitive symptoms from sulcation of the cortex. *Front. Neuroanat.* 15, 712862 <https://doi.org/10.3389/fnana.2021.712862>.
- Cardoso, M.J., Melbourne, A., Kendall, G.S., Modat, M., Robertson, N.J., Marlow, N., Ourselin, S., 2013. AdaPT: an adaptive preterm segmentation algorithm for neonatal brain MRI. *NeuroImage* 65, 97–108. <https://doi.org/10.1016/j.neuroimage.2012.08.009>.
- Chi, J.G., Dooling, E.C., Gilles, F.H., 1977a. Gyral development of the human brain. *Ann. Neurol.* 1, 86–93. <https://doi.org/10.1002/ana.4100110109>.
- Chi, J.G., Dooling, E.C., Gilles, F.H., 1977b. Left-right asymmetries of the temporal speech areas of the human foetus. *Arch. Neurol.* 34, 346–348. <https://doi.org/10.1001/archneur.1977.00500180040008>.
- Cordero-Grande, L., Hughes, E.J., Hutter, J., Price, A.N., Hajnal, J.V., 2018. Three-dimensional motion corrected sensitivity encoding reconstruction for multi-shot multi-slice MRI: Application to neonatal brain imaging: Aligned Multi-Shot Multi-Slice MRI. *Magn. Reson. Med.* 79, 1365–1376. <https://doi.org/10.1002/mrm.26796>.
- Coulon, O., Lefevre, J., Kloppel, S., Siebner, H., Mangin, J.-F., 2015. Quasi-isometric length parameterization of cortical sulci: Application to handedness and the central sulcus morphology, in: 2015 IEEE 12th International Symposium on Biomedical Imaging (ISBI). Presented at the 2015 IEEE 12th International Symposium on Biomedical Imaging (ISBI 2015), IEEE, Brooklyn, NY, USA, pp. 1268–1271. <https://doi.org/10.1109/ISBI.2015.7164105>.
- Cunningham, D.J., 1892. *Cunningham Memoirs - Contribution to the surface anatomy of the cerebral hemispheres by D.J. Cunningham with a chapter upon cranio-cerebral topography by Victor Horsley.*
- De Vareilles, H., Riviere, D., Pascucci, M., Sun, Z.-Y., Fischer, C., Leroy, F., Tataranno, M.-L., Benders, M.J., Dubois, J., Mangin, J.-F., 2023. Exploring the emergence of morphological asymmetries around the brain's Sylvian fissure: a longitudinal study of shape variability in preterm infants. *Cereb. Cortex* bhac533. <https://doi.org/10.1093/cercor/bhac533>.
- Dehaene-Lambertz, G., Spelke, E.S., 2015. The infancy of the human brain. *Neuron* 88, 93–109. <https://doi.org/10.1016/j.neuron.2015.09.026>.
- Dehaene-Lambertz, G., Hertz-Pannier, L., Dubois, J., 2006. Nature and nurture in language acquisition: anatomical and functional brain-imaging studies in infants. *Trends Neurosci.* 29, 367–373. <https://doi.org/10.1016/j.tins.2006.05.011>.
- del Toro, D., Ruff, T., Cederfjäll, E., Villalba, A., Seyit-Bremer, G., Borrell, V., Klein, R., 2017. Regulation of cerebral cortex folding by controlling neuronal migration via FLRT Adhesion Molecules. *Cell* 169 (621–635), e16. <https://doi.org/10.1016/j.cell.2017.04.012>.
- Duan, D., Xia, S., Rekik, I., Meng, Y., Wu, Z., Wang, L., Lin, W., Gilmore, J.H., Shen, D., Li, G., 2019. Exploring folding patterns of infant cerebral cortex based on multi-view curvature features: Methods and applications. *NeuroImage* 185, 575–592. <https://doi.org/10.1016/j.neuroimage.2018.08.041>.
- Dubois, J., 2021. Multimodal MRI: Applications to early brain development in infants. In: *Advances in Magnetic Resonance Technology and Applications*. Elsevier, pp. 153–176. <https://doi.org/10.1016/B978-0-12-816633-8.00017-X>.
- Dubois, J., Dehaene-Lambertz, G., 2015. foetal and Postnatal Development of the Cortex: MRI and Genetics. In: *Brain Mapping*. Elsevier, pp. 11–19. <https://doi.org/10.1016/B978-0-12-397025-1.00194-9>.
- Dubois, J., Benders, M., Cachia, A., Lazeyras, F., Ha-Vinh Leuchter, R., Sizonenko, S.V., Borradori-Tolsa, C., Mangin, J.F., Hüppi, P.S., 2008a. Mapping the Early Cortical Folding Process in the Preterm Newborn Brain. *Cereb. Cortex* 18, 1444–1454. <https://doi.org/10.1093/cercor/bhm180>.
- Dubois, J., Benders, M., Borradori-Tolsa, C., Cachia, A., Lazeyras, F., Ha-Vinh Leuchter, R., Sizonenko, S.V., Warfield, S.K., Mangin, J.F., Hüppi, P.S., 2008b. Primary cortical folding in the human newborn: an early marker of later functional development. *Brain* 131, 2028–2041. <https://doi.org/10.1093/brain/awn137>.
- Dubois, J., Benders, M., Lazeyras, F., Borradori-Tolsa, C., Leuchter, R.H.-V., Mangin, J.F., Hüppi, P.S., 2010. Structural asymmetries of perisylvian regions in the preterm newborn. *NeuroImage* 52, 32–42. <https://doi.org/10.1016/j.neuroimage.2010.03.054>.
- Dubois, J., Dehaene-Lambertz, G., Kulikova, S., Poupon, C., Hüppi, P.S., Hertz-Pannier, L., 2014. The early development of brain white matter: a review of imaging studies in foetuses, newborns and infants. *Neuroscience* 276, 48–71. <https://doi.org/10.1016/j.neuroscience.2013.12.044>.
- Dubois, J., Lefevre, J., Angleys, H., Leroy, F., Fischer, C., Lebenberg, J., Dehaene-Lambertz, G., Borradori-Tolsa, C., Lazeyras, F., Hertz-Pannier, L., Mangin, J.-F., Hüppi, P.S., Germanaud, D., 2019. The dynamics of cortical folding waves and prematurity-related deviations revealed by spatial and spectral analysis of gyrification. *NeuroImage* 185, 934–946. <https://doi.org/10.1016/j.neuroimage.2018.03.005>.
- Dubois, J., Alison, M., Counsell, S.J., Hertz-Pannier, L., Hüppi, P.S., Benders, M.J.N.L., 2021. MRI of the Neonatal Brain: A Review of Methodological Challenges and Neuroscientific Advances. *J. Magn. Reson Imaging* 53, 1318–1343. <https://doi.org/10.1002/jmri.27192>.
- Engelhardt, E., Inder, T.E., Alexopoulos, D., Dierker, D.L., Hill, J., Essen, D., Neil, J.J., 2015. Regional impairments of cortical folding in premature infants. *Ann. Neurol.* 77, 154–162. <https://doi.org/10.1002/ana.24313>.
- Feess-Higgins, A., Laroche, J.C., 1987. *Development of the Human Foetal Brain: an Anatomical Atlas*. Inserm-CNRS, Masson.
- Fernández, V., Llinares-Benadero, C., Borrell, V., 2016. Cerebral cortex expansion and folding: what have we learned. *EMBO J.* 35, 1021–1044. <https://doi.org/10.15252/embj.201593701>.
- Fish, A.M., Cachia, A., Fischer, C., Mankiw, C., Reardon, P.K., Clasen, L.S., Blumenthal, J. D., Greenstein, D., Giedd, J.N., Mangin, J.-F., Raznahan, A., 2016. Influences of brain size, sex, and sex chromosome complement on the architecture of human cortical folding. *Cereb. Cortex* cercor bhw323v1. <https://doi.org/10.1093/cercor/bhw323>.
- Foubet, O., Trejo, M., Toro, R., 2019. Mechanical morphogenesis and the development of neocortical organisation. *Cortex* 118, 315–326. <https://doi.org/10.1016/j.cortex.2018.03.005>.
- Garcia, K.E., Kroenke, C.D., Bayly, P.V., 2018a. Mechanics of cortical folding: stress, growth and stability. *Philos. Trans. R. Soc. B* 373, 20170321. <https://doi.org/10.1098/rstb.2017.0321>.
- Garcia, K.E., Robinson, E.C., Alexopoulos, D., Dierker, D.L., Glasser, M.F., Coalson, T.S., Ortinau, C.M., Rueckert, D., Taber, L.A., Van Essen, D.C., Rogers, C.E., Smyser, C.D., Bayly, P.V., 2018b. Dynamic patterns of cortical expansion during folding of the preterm human brain. *Proc. Natl. Acad. Sci. USA* 115, 3156–3161. <https://doi.org/10.1073/pnas.1715451115>.
- Garel, C., Chantrel, E., Brisse, H., Elmaleh, M., Luton, D., Oury, J.-F., Sebag, G., Hassan, M., 2001. foetal Cerebral Cortex: Normal Gestational Landmarks Identified Using Prenatal MR Imaging 6.
- Gay, O., Plaze, M., Oppenheim, C., Gaillard, R., Olié, J.-P., Krebs, M.-O., Cachia, A., 2017. Cognitive control deficit in patients with first-episode schizophrenia is associated with complex deviations of early brain development. *In: JPN*, 42, pp. 87–94. <https://doi.org/10.1503/jpn.150267>.
- Germanaud, D., Lefevre, J., Toro, R., Fischer, C., Dubois, J., Hertz-Pannier, L., Mangin, J.-F., 2012. Larger is twistier: Spectral analysis of gyrification (SPANGY) applied to adult brain size polymorphism. *NeuroImage* 63, 1257–1272. <https://doi.org/10.1016/j.neuroimage.2012.07.053>.
- Germann, J., Chakravarty, M.M., Collins, L.D., Petrides, M., 2019. Tight Coupling between Morphological Features of the Central Sulcus and Somatomotor Body Representations: A Combined Anatomical and Functional MRI Study. *Cereb. Cortex* bhz208. <https://doi.org/10.1093/cercor/bhz208>.
- Gholipour, A., Estroff, J.A., Barnewolt, C.E., Connolly, S.A., Warfield, S.K., 2011. foetal brain volumetry through MRI volumetric reconstruction and segmentation. *Int. J. CARS* 6, 329–339. <https://doi.org/10.1007/s11548-010-0512-x>.
- Ginsberg, Y., Ganor-Ariav, O., Hussein, H., Adam, D., Khatib, N., Weiner, Z., Beloosesky, R., Goldstein, I., 2021. Quantification of foetal Gyrogenesis in the Third Trimester. A Novel Algorithm for Evaluating foetal Sulci Development. *J. Neuroimaging* 31, 372–378. <https://doi.org/10.1111/jon.12817>.
- Glasel, H., Leroy, F., Dubois, J., Hertz-Pannier, L., Mangin, J.F., Dehaene-Lambertz, G., 2011. A robust cerebral asymmetry in the infant brain: The rightward superior temporal sulcus. *NeuroImage* 58, 716–723. <https://doi.org/10.1016/j.neuroimage.2011.06.016>.
- Gui, L., Lisowski, R., Faundez, T., Hüppi, P.S., Lazeyras, F., Kocher, M., 2012. Morphology-driven automatic segmentation of MR images of the neonatal brain. *Med. Image Anal.* 16, 1565–1579. <https://doi.org/10.1016/j.media.2012.07.006>.
- Habas, P.A., Kim, K., Corbett-Detig, J.M., Rousseau, F., Glenn, O.A., Barkovich, A.J., Studholme, C., 2010. A spatiotemporal atlas of MR intensity, tissue probability and shape of the foetal brain with application to segmentation. *NeuroImage* 53, 460–470. <https://doi.org/10.1016/j.neuroimage.2010.06.054>.

- Habas, P.A., Scott, J.A., Roosta, A., Rajagopalan, V., Kim, K., Rousseau, F., Barkovich, A. J., Glenn, O.A., Studholme, C., 2012. Early Folding Patterns and Asymmetries of the Normal Human Brain Detected from in Utero MRI. *Cereb. Cortex* 22, 13–25. <https://doi.org/10.1093/cercor/bhr053>.
- Hansen, P., Ballesteros, M., Soila, K., Garcia, L., Howard, J.M., 1993. MR imaging of the developing human brain. *RadioGraphics* 13, 21–36.
- Hedderich, D.M., Bäuml, J.G., Berndt, M.T., Menegaux, A., Scheef, L., Daamen, M., Zimmer, C., Bartmann, P., Boecker, H., Wolke, D., Gaser, C., Sorg, C., 2019. Aberrant gyrification contributes to the link between gestational age and adult IQ after premature birth. *Brain* 142, 1255–1269. <https://doi.org/10.1093/brain/awz071>.
- Heuer, K., Toro, R., 2019. Role of mechanical morphogenesis in the development and evolution of the neocortex. *Phys. Life Rev.* 31, 233–239. <https://doi.org/10.1016/j.plrev.2019.01.012>.
- Hill, J., Inder, T., Neil, J., Dierker, D., Harwell, J., Van Essen, D., 2010. Similar patterns of cortical expansion during human development and evolution. *Proc. Natl. Acad. Sci.* 107, 13135–13140. <https://doi.org/10.1073/pnas.1001229107>.
- Im, K., Grant, P.E., 2019. Sulcal pits and patterns in developing human brains. *NeuroImage* 185, 881–890. <https://doi.org/10.1016/j.neuroimage.2018.03.057>.
- Im, K., Lee, J.-M., Lyttelton, O., Kim, S.H., Evans, A.C., Kim, S.I., 2008. Brain size and cortical structure in the adult human brain. *Cereb. Cortex* 18, 2181–2191. <https://doi.org/10.1093/cercor/bhm244>.
- Im, K., Jo, H.J., Mangin, J.-F., Evans, A.C., Kim, S.I., Lee, J.-M., 2010. Spatial distribution of deep sulcal landmarks and hemispherical asymmetry on the cortical surface. *Cereb. Cortex* 20, 602–611. <https://doi.org/10.1093/cercor/bhp127>.
- Im, K., Pienaar, R., Lee, J.-M., Seong, J.-K., Choi, Y.Y., Lee, K.H., Grant, P.E., 2011. Quantitative comparison and analysis of sulcal patterns using sulcal graph matching: A twin study. *NeuroImage* 57, 1077–1086. <https://doi.org/10.1016/j.neuroimage.2011.04.062>.
- Im, K., Guimaraes, A., Kim, Y., Cottrill, E., Gagoski, B., Rollins, C., Ortinau, C., Yang, E., Grant, P.E., 2017. Quantitative folding pattern analysis of early primary sulci in human fetuses with brain abnormalities. *AJNR Am. J. Neuroradiol.* 38, 1449–1455. <https://doi.org/10.3174/ajnr.A5217>.
- Işgum, I., Benders, M.J.N.L., Avants, B., Cardoso, M.J., Counsell, S.J., Gomez, E.F., Gui, L., Hüppi, P.S., Kersbergen, K.J., Makropoulos, A., Melbourne, A., Moeskops, P., Mol, C.P., Kuklisova-Murgasova, M., Rueckert, D., Schnabel, J.A., Srhoj-Egkher, V., Wu, J., Wang, S., de Vries, L.S., Viergever, M.A., 2015. Evaluation of automatic neonatal brain segmentation algorithms: The NeoBrainS12 challenge. *Med. Image Anal.* 20, 135–151. <https://doi.org/10.1016/j.media.2014.11.001>.
- Jiang, X., Zhang, T., Zhang, S., Kendrick, K.M., Liu, T., 2021. Fundamental functional differences between gyri and sulci: implications for brain function, cognition, and behavior. *Psychoradiology* 1, 23–41. <https://doi.org/10.1093/psyrad/kkab002>.
- Kapellou, O., Counsell, S.J., Kennea, N., Dyet, L., Saeed, N., Stark, J., Maalouf, E., Duggan, P., Ajayi-Obe, M., Hajnal, J., Allsop, J.M., Boardman, J., Rutherford, M.A., Cowan, F., Edwards, A.D., 2006. Abnormal cortical development after premature birth shown by altered allometric scaling of brain growth. *PLoS Med* 3, e265. <https://doi.org/10.1371/journal.pmed.0030265>.
- Kersbergen, K.J., Leroy, F., Işgum, I., Groenendaal, F., de Vries, L.S., Claessens, N.H.P., van Haastert, I.C., Moeskops, P., Fischer, C., Mangin, J.-F., Viergever, M.A., Dubois, J., Benders, M.J.N.L., 2016. Relation between clinical risk factors, early cortical changes, and neurodevelopmental outcome in preterm infants. *NeuroImage* 142, 301–310. <https://doi.org/10.1016/j.neuroimage.2016.07.010>.
- Kim, H., Lepage, C., Maheshwary, R., Jeon, S., Evans, A.C., Hess, C.P., Barkovich, A.J., Xu, D., 2016b. NEOCIVET: towards accurate morphometry of neonatal gyrification and clinical applications in preterm newborns. *NeuroImage* 138, 28–42. <https://doi.org/10.1016/j.neuroimage.2016.05.034>.
- Kim, S.H., Lyu, L., Fonov, V.S., Vachet, C., Hazlett, H.C., Smith, R.G., Piven, J., Dager, S. R., Mckinstry, R.C., Pruettt, J.R., Evans, A.C., Collins, D.L., Botteron, K.N., Schultz, R. T., Gerig, G., Styner, M.A., 2016a. Development of cortical shape in the human brain from 6 to 24 months of age via a novel measure of shape complexity. *NeuroImage* 135, 163–176. <https://doi.org/10.1016/j.neuroimage.2016.04.053>.
- Kim, S.Y., Liu, M., Hong, S.-J., Toga, A.W., Barkovich, A.J., Xu, D., Kim, H., 2020. Disruption and compensation of sulcation-based covariance networks in neonatal brain growth after perinatal injury. *Cereb. Cortex* bhaa181. <https://doi.org/10.1093/cercor/bhaa181>.
- Kochunov, P., Mangin, J.-F., Coyle, T., Lancaster, J., Thompson, P., Rivière, D., Cointepas, Y., Régis, J., Schlosser, A., Royall, D.R., Zilles, K., Mazziotta, J., Toga, A., Fox, P.T., 2005. Age-related morphology trends of cortical sulci. *Hum. Brain Mapp.* 26, 210–220. <https://doi.org/10.1002/hbm.20198>.
- Kostović, I., Sedmak, G., Judaš, M., 2019. Neural histology and neurogenesis of the human foetal and infant brain. *NeuroImage* 188, 743–773. <https://doi.org/10.1016/j.neuroimage.2018.12.043>.
- Kronke, C.D., Bayly, P.V., 2018. How Forces Fold the Cerebral Cortex. *J. Neurosci.* 38, 767–775. <https://doi.org/10.1523/JNEUROSCI.1105-17.2017>.
- Kuklisova-Murgasova, M., Quaghebeur, G., Rutherford, M.A., Hajnal, J.V., Schnabel, J. A., 2012. Reconstruction of foetal brain MRI with intensity matching and complete outlier removal. *Med. Image Anal.* 16, 1550–1564. <https://doi.org/10.1016/j.media.2012.07.004>.
- Lavoie, S., Bartholomeuz, C.F., Nelson, B., Lin, A., McGorry, P.D., Velakoulis, D., Whittle, S.L., Yung, A.R., Pantelis, C., Wood, S.J., 2014. Sulcogyral pattern and sulcal count of the orbitofrontal cortex in individuals at ultra high risk for psychosis. *Schizophr. Res.* 154, 93–99. <https://doi.org/10.1016/j.schres.2014.02.008>.
- Le Guen, Y., Leroy, F., Auzias, G., Rivière, D., Grigis, A., Mangin, J.-F., Coulon, O., Dehaene-Lambertz, G., Frouin, V., 2018. The chaotic morphology of the left superior temporal sulcus is genetically constrained. *NeuroImage* 174, 297–307. <https://doi.org/10.1016/j.neuroimage.2018.03.046>.
- Le Guen, Y., Leroy, F., Philippe, C., Imagen, consortium, Mangin, J.-F., Dehaene-Lambertz, G., Frouin, V., 2019. Enhancer locus in ch14q23.1 modulates brain asymmetric temporal regions involved in language processing. *Neuroscience*. <https://doi.org/10.1101/539189>.
- Lebenberg, J., Labit, M., Auzias, G., Mohlberg, H., Fischer, C., Rivière, D., Duchesnay, E., Kabdebon, C., Leroy, F., Labra, N., Poupon, F., Dickscheid, T., Hertz-Pannier, L., Poupon, C., Dehaene-Lambertz, G., Hüppi, P., Amunts, K., Dubois, J., Mangin, J.-F., 2018. A framework based on sulcal constraints to align preterm, infant and adult human brain images acquired in vivo and post mortem. *Brain Struct. Funct.* 223, 4153–4168. <https://doi.org/10.1007/s00429-018-1735-9>.
- Lebenberg, J., Mangin, J.-F., Thirion, B., Poupon, C., Hertz-Pannier, L., Leroy, F., Adibpour, P., Dehaene-Lambertz, G., Dubois, J., 2019. Mapping the asynchrony of cortical maturation in the infant brain: A MRI multi-parametric clustering approach. *NeuroImage* 185, 641–653. <https://doi.org/10.1016/j.neuroimage.2018.07.022>.
- Lefèvre, J., Mangin, J.-F., 2010. A reaction-diffusion model of human brain development. *PLoS Comput. Biol.* 6, e1000749. <https://doi.org/10.1371/journal.pcbi.1000749>.
- Lefèvre, J., Germanaud, D., Dubois, J., Rousseau, F., de Macedo Santos, I., Angleys, H., Mangin, J.-F., Hüppi, P.S., Girard, N., De Guio, F., 2016. Are developmental trajectories of cortical folding comparable between cross-sectional datasets of fetuses and preterm newborns? *Cereb. Cortex* 26, 3023–3035. <https://doi.org/10.1093/cercor/bhv123>.
- Lefèvre, J., Pepe, A., Muscato, J., De Guio, F., Girard, N., Auzias, G., Germanaud, D., 2018. SPANOL (Spectral Analysis of Lobes): a spectral clustering framework for individual and group parcellation of cortical surfaces in lobes. *Front. Neurosci.* 12, 354. <https://doi.org/10.3389/fnins.2018.00354>.
- Leroy, F., Mangin, J.-F., Rousseau, F., Glasel, H., Hertz-Pannier, L., Dubois, J., Dehaene-Lambertz, G., 2011. Atlas-Free Surface Reconstruction of the Cortical Grey-White Interface in Infants. *PLoS ONE* 6, e27128. <https://doi.org/10.1371/journal.pone.0027128>.
- Leroy, F., Cai, Q., Bogart, S.L., Dubois, J., Coulon, O., Monzalvo, K., Fischer, C., Glasel, H., Van der Haegen, L., Bénézit, A., Lin, C.-P., Kennedy, D.N., Ihara, A.S., Hertz-Pannier, L., Moutard, M.-L., Poupon, C., Brysbaert, M., Roberts, N., Hopkins, W.D., Mangin, J.-F., Dehaene-Lambertz, G., 2015. New human-specific brain landmark: The depth asymmetry of superior temporal sulcus. *Proc. Natl. Acad. Sci. USA* 112, 1208–1213. <https://doi.org/10.1073/pnas.1412389112>.
- Lewitus, E., Kelava, I., Huttner, W.B., 2013. Conical expansion of the outer subventricular zone and the role of neocortical folding in evolution and development. *Front. Hum. Neurosci.* 7. <https://doi.org/10.3389/fnhum.2013.00424>.
- Li, G., Wang, L., Shi, F., Lyall, A.E., Lin, W., Gilmore, J.H., Shen, D., 2014. Mapping longitudinal development of local cortical gyrification in infants from birth to 2 Years of age. *J. Neurosci.* 34, 4228–4238. <https://doi.org/10.1523/JNEUROSCI.3976-13.2014>.
- Li, G., Wang, L., Yap, P.-T., Wang, F., Wu, Z., Meng, Y., Dong, P., Kim, J., Shi, F., Rekić, I., Lin, W., Shen, D., 2019. Computational neuroanatomy of baby brains: a review. *NeuroImage* 185, 906–925. <https://doi.org/10.1016/j.neuroimage.2018.03.042>.
- Liu, M., Kitsch, A., Miller, S., Chau, V., Poskitt, K., Rousseau, F., Shaw, D., Studholme, C., 2016. Patch-based augmentation of Expectation–Maximization for brain MRI tissue segmentation at arbitrary age after premature birth. *NeuroImage* 127, 387–408. <https://doi.org/10.1016/j.neuroimage.2015.12.009>.
- Llinares-Benadero, C., Borrell, V., 2019. Deconstructing cortical folding: genetic, cellular and mechanical determinants. *Nat. Rev. Neurosci.* 20, 161–176. <https://doi.org/10.1038/s41583-018-0112-2>.
- Lohmann, G., von Cramon, D.Y., Colchester, A.C.F., 2008. Deep sulcal landmarks provide an organizing framework for human cortical folding. *Cereb. Cortex* 18, 1415–1420. <https://doi.org/10.1093/cercor/bhm174>.
- Luders, E., Thompson, P.M., Narr, K.L., Toga, A.W., Jancke, L., Gaser, C., 2006. A curvature-based approach to estimate local gyrification on the cortical surface. *NeuroImage* 29, 1224–1230. <https://doi.org/10.1016/j.neuroimage.2005.08.049>.
- Makropoulos, A., Gousias, I.S., Ledig, C., Aljabar, P., Serag, A., Hajnal, J.V., Edwards, A. D., Counsell, S.J., Rueckert, D., 2014. Automatic Whole Brain MRI Segmentation of the Developing Neonatal Brain. *IEEE Trans. Med. Imaging* 33, 1818–1831. <https://doi.org/10.1109/TMI.2014.2322280>.
- Makropoulos, A., Robinson, E.C., Schuh, A., Wright, R., Fitzgibbon, S., Bozek, J., Counsell, S.J., Steinweg, J., Vecchiato, K., Passerat-Palmbach, J., Lenz, G., Mortari, F., Tenev, T., Duff, E.P., Bastiani, M., Cordero-Grande, L., Hughes, E., Tumor, N., Tournier, J.-D., Hutter, J., Price, A.N., Teixeira, R.P.A.G., Murgasova, M., Victor, S., Kelly, C., Rutherford, M.A., Smith, S.M., Edwards, A.D., Hajnal, J.V., Jenkinson, M., Rueckert, D., 2018a. The developing human connectome project: A minimal processing pipeline for neonatal cortical surface reconstruction. *NeuroImage* 173, 88–112. <https://doi.org/10.1016/j.neuroimage.2018.01.054>.
- Makropoulos, A., Counsell, S.J., Rueckert, D., 2018b. A review on automatic foetal and neonatal brain MRI segmentation. *NeuroImage* 170, 231–248. <https://doi.org/10.1016/j.neuroimage.2017.06.074>.
- Mallela, A.N., Deng, H., Brisbin, A.K., Bush, A., Goldschmidt, E., 2020. Sylvian fissure development is linked to differential genetic expression in the pre-folded brain. *Sci. Rep.* 10, 14489. <https://doi.org/10.1038/s41598-020-71535-4>.
- Mangin, J.-F., Jouvent, E., Cachia, A., 2010. vivo Meas. cortical Morphol.: means Mean.: *Curr. Opin. Neurol.* 1. <https://doi.org/10.1097/WCO.0b013e32833a0a0c>.
- Mangin, J.-F., Auzias, G., Coulon, O., Sun, Z.Y., Rivière, D., Régis, J., 2015a. Sulci as Landmarks. In: *Brain Mapping*. Elsevier, pp. 45–52. <https://doi.org/10.1016/B978-0-12-397025-1.00198-6>.
- Mangin, J.-F., Perrot, M., Operto, G., Cachia, A., Fischer, C., Lefèvre, J., Rivière, D., 2015b. Sulcus Identification and labelling. In: *Brain Mapping*. Elsevier, pp. 365–371. <https://doi.org/10.1016/B978-0-12-397025-1.00307-9>.

- Mangin, J.-F., Leberberg, J., Lefranc, S., Labra, N., Auzias, G., Labit, M., Guevara, M., Mohlberg, H., Roca, P., Guevara, P., Dubois, J., Leroy, F., Dehaene-Lambertz, G., Cachia, A., Dickscheid, T., Coulon, O., Poupon, C., Rivière, D., Amunts, K., Sun, Z.Y., 2016. Spatial normalization of brain images and beyond. *Med. Image Anal.* 33, 127–133. <https://doi.org/10.1016/j.media.2016.06.008>.
- Massimo, M., Long, K.R., 2022. Orchestrating human neocortex development across the scales; from micro to macro. *Semin. Cell Dev. Biol.* 130, 24–36. <https://doi.org/10.1016/j.semcdb.2021.09.007>.
- Meng, Y., Li, G., Lin, W., Gilmore, J.H., Shen, D., 2014. Spatial distribution and longitudinal development of deep cortical sulcal landmarks in infants. *NeuroImage* 100, 206–218. <https://doi.org/10.1016/j.neuroimage.2014.06.004>.
- Meng, Y., Li, G., Wang, L., Lin, W., Gilmore, J.H., Shen, D., 2018. Discovering cortical sulcal folding patterns in neonates using large-scale dataset. *Hum. Brain Mapp.* 39, 3625–3635. <https://doi.org/10.1002/hbm.24199>.
- Moeskops, P., Benders, M.J.N.L., Kersbergen, K.J., Groenendaal, F., de Vries, L.S., Vierveger, M.A., Išgum, I., 2015. Development of Cortical Morphology Evaluated with Longitudinal MR Brain Images of Preterm Infants. *PLoS ONE* 10, e0131552. <https://doi.org/10.1371/journal.pone.0131552>.
- Ono, M., Kubik, S., & Abernathy, C.D. (1990). *Atlas of the cerebral sulci*. Thieme Medical Publishers.
- Orasanu, E., Melbourne, A., Cardoso, M.J., Lomabert, H., Kendall, G.S., Robertson, N.J., Marlow, N., Ourselin, S., 2016. Cortical folding of the preterm brain: a longitudinal analysis of extremely preterm born neonates using spectral matching. *Brain Behav.* 6, e00488. <https://doi.org/10.1002/brb3.488>.
- Padilla, N., Alexandrou, G., Blennow, M., Lagercrantz, H., Ådén, U., 2015. Brain growth gains and losses in extremely preterm infants at term. *Cereb. Cortex* 25, 1897–1905. <https://doi.org/10.1093/cercor/bht431>.
- Papini, C., Palaniyappan, L., Kroll, J., Froudist-Walsh, S., Murray, R.M., Nosarti, C., 2020. Altered Cortical Gyrfication in Adults Who Were Born Very Preterm and Its Associations With Cognition and Mental Health. *Biol. Psychiatry: Cogn. Neurosci. Neuroimaging* 5, 640–650. <https://doi.org/10.1016/j.bpsc.2020.01.006>.
- Payette, K., de Dumast, P., Kebiri, H., Ezhov, I., Paetzold, J.C., Shit, S., Iqbal, A., Khan, R., Kottke, R., Grethen, P., Ji, H., Lanczi, L., Nagy, M., Beresova, M., Nguyen, T.D., Natalucci, G., Karayannis, T., Menze, B., Bach Cuadra, M., Jakab, A., 2021. An automatic multi-tissue human foetal brain segmentation benchmark using the foetal Tissue Annotation Dataset. *Sci. Data* 8, 167. <https://doi.org/10.1038/s41597-021-00946-3>.
- Perrot, M., Rivière, D., Mangin, J.-F., 2011. Cortical sulci recognition and spatial normalization. *Med. Image Anal.* 15, 529–550. <https://doi.org/10.1016/j.media.2011.02.008>.
- Petrides, M., 2019. *Atlas of the morphology of the human cerebral cortex on the average MNI brain*. Academic Press, New York.
- Piao, X., Hill, R.S., Bodell, A., Chang, B.S., Basel-Vanagaite, L., Straussberg, R., Dobyns, W.B., Qasrawi, B., Winter, R.M., Innes, A.M., Voit, T., Ross, M.E., Michaud, J.L., Descarrie, J.-C., Barkovich, A.J., Walsh, C.A., 2004. G Protein-Coupled Receptor-Dependent Development of Human Frontal Cortex. *Science* 303, 2033–2036. <https://doi.org/10.1126/science.1092780>.
- Pizzagalli, F., Auzias, G., Yang, Q., Mathias, S.R., Faskowitz, J., Boyd, J.D., Amini, A., Rivière, D., McMahon, K.L., de Zubicaray, G.I., Martin, N.G., Mangin, J.-F., Glahn, D. C., Blangero, J., Wright, M.J., Thompson, P.M., Kochunov, P., Jahanshad, N., 2020. The reliability and heritability of cortical folds and their genetic correlations across hemispheres. *Commun. Biol.* 3, 510. <https://doi.org/10.1038/s42003-020-01163-1>.
- Prastawa, M., Gilmore, J.H., Lin, W., Gerig, G., 2005. Automatic segmentation of MR images of the developing newborn brain. *Med. Image Anal.* 9, 457–466. <https://doi.org/10.1016/j.media.2005.05.007>.
- Rakic, P., 1988. Specification of cerebral cortical areas. *Science* 241, 170–176. <https://doi.org/10.1126/science.3291116>.
- Rana, S., Shishegar, R., Quezada, S., Johnston, L., Walker, D.W., Tolcos, M., 2019. The subplate: a potential driver of cortical folding. *Cereb. Cortex* 29, 4697–4708. <https://doi.org/10.1093/cercor/bhz003>.
- Régis, J., Mangin, J.-F., Ochiai, T., Frouin, V., Rivière, D., Cachia, A., Tamura, M., Samson, Y., 2005. “Sulcal Root” Generic Model: a Hypothesis to Overcome the Variability of the Human Cortex Folding Patterns. *Neurol. Med. Chir. (Tokyo)* 45, 1–17. <https://doi.org/10.2176/nmc.45.1>.
- Rekik, I., Li, G., Lin, W., Shen, D., 2018. Do Baby Brain Cortices that Look Alike at Birth Grow Alike During the First Year of Postnatal Development? In: Frangi, A.F., Schnabel, J.A., Davatzikos, C., Alberola-López, C., Fichtinger, G. (Eds.), *Medical Image Computing and Computer Assisted Intervention – MICCAI 2018*. Springer International Publishing, Cham, pp. 566–574. https://doi.org/10.1007/978-3-030-00931-1_65.
- Robinson, E.C., Garcia, K., Glasser, M.F., Chen, Z., Coalson, T.S., Makropoulos, A., Bozek, J., Wright, R., Schuh, A., Webster, M., Hutter, J., Price, A., Cordero Grande, L., Hughes, E., Tusor, N., Bayly, P.V., Van Essen, D.C., Smith, S.M., Edwards, A.D., Hajnal, J., Jenkinson, M., Glocker, B., Rueckert, D., 2018. Multimodal surface matching with higher-order smoothness constraints. *NeuroImage* 167, 453–465. <https://doi.org/10.1016/j.neuroimage.2017.10.037>.
- Rockel, A.J., Hiorns, R.W., Powell, T.P.S., 1980. The basic uniformity in structure of the neocortex. In: *Brain*, 103, pp. 221–244. <https://doi.org/10.1093/brain/103.2.221>.
- Ronan, L., Fletcher, P.C., 2015. From genes to folds: a review of cortical gyrfication theory. *Brain Struct. Funct.* 220, 2475–2483. <https://doi.org/10.1007/s00429-014-0961-z>.
- Rousseau, F., Glenn, O.A., Iordanova, B., Rodriguez-Carranza, C., Vigneron, D.B., Barkovich, J.A., Studholme, C., 2006. Registration-Based Approach for Reconstruction of High-Resolution In Utero foetal MR Brain Images. *Acad. Radiol.* 13, 1072–1081. <https://doi.org/10.1016/j.acra.2006.05.003>.
- Rousseau, F., Oubel, E., Pontabry, J., Schweitzer, M., Studholme, C., Koob, M., Dietemann, J.-L., 2013. BTK: An open-source toolkit for foetal brain MR image processing. *Comput. Methods Prog. Biomed.* 109, 65–73. <https://doi.org/10.1016/j.cmpb.2012.08.007>.
- Sarrazin, S., Cachia, A., Hozer, F., McDonald, C., Emsell, L., Cannon, D.M., Wessa, M., Linke, J., Versace, A., Hamdani, N., D’Albis, M.-A., Delavest, M., Phillips, M.L., Brambilla, P., Bellani, M., Polosan, M., Favre, P., Leboyer, M., Mangin, J.-F., Houenou, J., 2018. Neurodevelopmental subtypes of bipolar disorder are related to cortical folding patterns: An international multicenter study. *Bipolar Disord.* 20, 721–732. <https://doi.org/10.1111/bdi.12664>.
- Shi, F., Fan, Y., Tang, S., Gilmore, J.H., Lin, W., Shen, D., 2010. Neonatal brain image segmentation in longitudinal MRI studies. *NeuroImage* 49, 391–400. <https://doi.org/10.1016/j.neuroimage.2009.07.066>.
- Shimony, J.S., Smyser, C.D., Wideman, G., Alexopoulos, D., Hill, J., Harwell, J., Dierker, D., Van Essen, D.C., Inder, T.E., Neil, J.J., 2016. Comparison of cortical folding measures for evaluation of developing human brain. *NeuroImage* 125, 780–790. <https://doi.org/10.1016/j.neuroimage.2015.11.001>.
- Sowell, E.R., Thompson, P.M., Rex, D., Kornsand, D., Tessner, K.D., Jernigan, T.L., Toga, A.W., 2002. Mapping sulcal pattern asymmetry and local cortical surface gray matter distribution in vivo: maturation in perisylvian cortices. *Cereb. Cortex* 12, 17–26. <https://doi.org/10.1093/cercor/12.1.17>.
- Sprung-Much, T., Petrides, M., 2018. Morphological patterns and spatial probability maps of two defining sulci of the posterior ventrolateral frontal cortex of the human brain: the sulcus diagonalis and the anterior ascending ramus of the lateral fissure. *Brain Struct. Funct.* 223, 4125–4152. <https://doi.org/10.1007/s00429-018-1733-y>.
- Striedter, G.F., Srinivasan, S., Monuki, E.S., 2015. Cortical folding: when, where, how, and why? *Annu. Rev. Neurosci.* 38, 291–307. <https://doi.org/10.1146/annurev-neuro-071714-034128>.
- Studholme, C., 2015. Mapping the developing human brain in utero using quantitative MR imaging techniques. *Semin. Perinatol.* 39, 105–112. <https://doi.org/10.1053/j.semper.2015.01.003>.
- Sun, Z.Y., Klöppel, S., Rivière, D., Perrot, M., Frackowiak, R., Siebner, H., Mangin, J.-F., 2012. The effect of handedness on the shape of the central sulcus. *NeuroImage* 60, 332–339. <https://doi.org/10.1016/j.neuroimage.2011.12.050>.
- Sun, Z.Y., Pinel, P., Rivière, D., Moreno, A., Dehaene, S., Mangin, J.-F., 2016. Linking morphological and functional variability in hand movement and silent reading. *Brain Struct. Funct.* 221, 3361–3371. <https://doi.org/10.1007/s00429-015-1106-8>.
- Sun, Z.Y., Cachia, A., Rivière, D., Fischer, C., Makin, T., Mangin, J.-F., 2017. Congenital unilateral upper limb absence flattens the contralateral hand-knob. Organization for Human Brain Mapping Meeting (OHBM 2017), Vancouver, Canada. (hal-02876124).
- Sur, M., Rubenstein, J.L.R., 2005. Patterning and plasticity of the cerebral cortex. *Science* 310, 805–810. <https://doi.org/10.1126/science.1112070>.
- Tallinen, T., Chung, J.Y., Biggins, J.S., Mahadevan, L., 2014. Gyrfication from constrained cortical expansion. *Proc. Natl. Acad. Sci.* 111, 12667–12672. <https://doi.org/10.1073/pnas.1406015111>.
- Tallinen, T., Chung, J.Y., Rousseau, F., Girard, N., Lefèvre, J., Mahadevan, L., 2016. On the growth and form of cortical convolutions. *Nat. Phys.* 12, 588–593. <https://doi.org/10.1038/nphys3632>.
- Tarui, T., Madan, N., Farhat, N., Kitano, R., Ceren Tanritanir, A., Graham, G., Gagoski, B., Craig, A., Rollins, C.K., Ortinau, C., Iyer, V., Pienaar, R., Bianchi, D.W., Grant, P.E., Im, K., 2018. Disorganized patterns of sulcal position in fetal brains with agenesis of corpus callosum. *Cereb. Cortex* 28, 3192–3203. <https://doi.org/10.1093/cercor/bhx191>.
- Tissier, C., Linzarini, A., Allaire-Duquette, G., Mevel, K., Poirel, N., Dollfus, S., Etard, O., Orliac, F., Peyrin, C., Charron, S., Raznahan, A., Houde, O., Borst, G., Cachia, A., 2018. Sulcal Polymorphisms of the IFC and ACC Contribute to Inhibitory Control Variability in Children and Adults. *ENEURO*.0197-17.2018. <https://doi.org/10.1523/ENEURO.0197-17.2018>.
- Toro, R., Burnod, Y., 2005. A morphogenetic model for the development of cortical convolutions. *Cereb. Cortex* 15, 1900–1913. <https://doi.org/10.1093/cercor/bhi068>.
- van der Knaap, M.S., van Wezel-Meijler, G., Barth, P.G., Barkhof, F., Adèr, H.J., Valk, J., 1996. Normal gyration and sulcation in preterm and term neonates: appearance on MR images. *Radiology*. <https://doi.org/10.1148/radiology.200.2.8685331>.
- Van Essen, D.C., 1997. A tension-based theory of morphogenesis and compact wiring in the central nervous system. *Nature* 385, 313–318. <https://doi.org/10.1038/385313a0>.
- Van Essen, D.C., 2020. A 2020 view of tension-based cortical morphogenesis. *PNAS* 117, 32868–32879. <https://doi.org/10.1073/pnas.2016830117>.
- Van Essen, D.C., Donahue, C.J., Coalson, T.S., Kennedy, H., Hayashi, T., Glasser, M.F., 2019. Cerebral cortical folding, parcellation, and connectivity in humans, nonhuman primates, and mice. *Proc. Natl. Acad. Sci. USA* 116, 26173–26180. <https://doi.org/10.1073/pnas.1902299116>.
- de Vareilles, H., Rivière, D., Sun, Z.-Y., Fischer, C., Leroy, F., Neumane, S., Stopar, N., Eijermans, R., Ballu, M., Tataranno, M.-L., Benders, M., Mangin, J.-F., Dubois, J., 2022. Shape variability of the central sulcus in the developing brain: a longitudinal descriptive and predictive study in preterm infants. *NeuroImage* 251, 118837. <https://doi.org/10.1016/j.neuroimage.2021.118837>.
- Vasung, L., Rollins, C.K., Yun, H.J., Velasco-Annis, C., Zhang, J., Wagstyl, K., Evans, A., Warfield, S.K., Feldman, H.A., Grant, P.E., Gholipour, A., 2019. Quantitative In vivo MRI assessment of structural asymmetries and sexual dimorphism of transient foetal compartments in the human brain. *Cereb. Cortex* bhz200. <https://doi.org/10.1093/cercor/bhz200>.
- Vasung, L., Zhao, C., Barkovich, M., Rollins, C.K., Zhang, J., Lepage, C., Corcoran, T., Velasco-Annis, C., Yun, H.J., Im, K., Warfield, S.K., Evans, A.C., Huang, H., Gholipour, A., Grant, P.E., 2021. Association between Quantitative MR Markers of

- Cortical Evolving Organization and Gene Expression during Human Prenatal Brain Development. *Cereb. Cortex* 31, 3610–3621. <https://doi.org/10.1093/cercor/bhab035>.
- Wang, L., Shi, F., Lin, W., Gilmore, J.H., Shen, D., 2011. Automatic segmentation of neonatal images using convex optimization and coupled level sets. *NeuroImage* 58, 805–817. <https://doi.org/10.1016/j.neuroimage.2011.06.064>.
- Wang, L., Gao, Y., Shi, F., Li, G., Gilmore, J.H., Lin, W., Shen, D., 2015. LINKS: Learning-based multi-source IntegratioN framework for Segmentation of infant brain images. *NeuroImage* 108, 160–172. <https://doi.org/10.1016/j.neuroimage.2014.12.042>.
- Wang, L., Yao, J., Hu, N., 2019. A mechanical method of cerebral cortical folding development based on thermal expansion. *Sci. Rep.* 9, 1914. <https://doi.org/10.1038/s41598-018-37461-2>.
- Wang, X., Studholme, C., Grigsby, P.L., Frias, A.E., Cuzon Carlson, V.C., Kroenke, C.D., 2017. Folding, But Not Surface Area Expansion, Is Associated with Cellular Morphological Maturation in the Fetal Cerebral Cortex. *J. Neurosci.* 37, 1971–1983. <https://doi.org/10.1523/JNEUROSCI.3157-16.2017>.
- Wang, X., Lefevre, J., Bohi, A., Harrach, M.A., Dinomais, M., Rousseau, F., 2021. The influence of biophysical parameters in a biomechanical model of cortical folding patterns. *Sci. Rep.* 11, 7686. <https://doi.org/10.1038/s41598-021-87124-y>.
- Welker, W., 1990. Why Does Cerebral Cortex Fissure and Fold? *Cereb. Cortex* 3–137.
- Wright, R., Kyriakopoulou, V., Ledig, C., Rutherford, M.A., Hajnal, J.V., Rueckert, D., Aljabar, P., 2014. Automatic quantification of normal cortical folding patterns from foetal brain MRI. *NeuroImage* 91, 21–32. <https://doi.org/10.1016/j.neuroimage.2014.01.034>.
- Wright, R., Makropoulos, A., Kyriakopoulou, V., Patkee, P.A., Koch, L.M., Rutherford, M.A., Hajnal, J.V., Rueckert, D., Aljabar, P., 2015. Construction of a foetal spatio-temporal cortical surface atlas from in utero MRI: Application of spectral surface matching. *NeuroImage* 120, 467–480. <https://doi.org/10.1016/j.neuroimage.2015.05.087>.
- Xia, J., Wang, F., Benkarim, O.M., Sanroma, G., Piella, G., González Ballester, M.A., Hahner, N., Eixarch, E., Zhang, C., Shen, D., Li, G., 2019. Fetal cortical surface atlas parcellation based on growth patterns. *Hum. Brain Mapp.* hbm 24637. <https://doi.org/10.1002/hbm.24637>.
- Xu, G., Knutsen, A.K., Dikranian, K., Kroenke, C.D., Bayly, P.V., Taber, L.A., 2010. Axons Pull on the Brain, But Tension Does Not Drive Cortical Folding. *J. Biomech. Eng.* 132, 071013 <https://doi.org/10.1115/1.4001683>.
- Yun, H.J., Chung, A.W., Vasung, L., Yang, E., Tarui, T., Rollins, C.K., Ortinau, C.M., Grant, P.E., Im, K., 2019. Automatic labelling of cortical sulci for the human foetal brain based on spatio-temporal information of gyrification. *NeuroImage* 188, 473–482. <https://doi.org/10.1016/j.neuroimage.2018.12.023>.
- Yun, H.J., Perez, J.D.R., Sosa, P., Valdés, J.A., Madan, N., Kitano, R., Akiyama, S., Skotko, B.G., Feldman, H.A., Bianchi, D.W., Grant, P.E., Tarui, T., Im, K., 2021. Regional Alterations in Cortical Sulcal Depth in Living Fetuses with Down Syndrome. *Cereb. Cortex* 31, 757–767. <https://doi.org/10.1093/cercor/bhaa255>.
- Zhao, F., Wu, Z., Li, G., 2022. Deep learning in cortical surface-based neuroimage analysis: a systematic review. S2667102622000493 *Intell. Med.* <https://doi.org/10.1016/j.imed.2022.06.002>.
- Zilles, K., Palomero-Gallagher, N., Amunts, K., 2013. Development of cortical folding during evolution and ontogeny. *Trends Neurosci.* 36, 275–284. <https://doi.org/10.1016/j.tins.2013.01.006>.